arXiv:cond-mat/0512288v2 [cond-mat.str-el] 18 Jan 2007

Relationship between the thermopower and entropy of strongly correlated electron systems

V. Zlatić[1,2], R. Monnier[3], J. Freericks[4], K. W. Becker[2]
[1]*Institute of Physics, Bijenička c. 46, 10001 Zagreb, Croatia (permanent address)*
[2]*Institut für Theoretische Physik, Technische Universität Dresden, 01062 Dresden, Germany*
[3]*ETH Hönggerberg, Laboratorium für Festkörperphysik, 8093 Zürich, Switzerland and*
[4]*Georgetown University, Washington D.C., USA*
(Dated: March 23, 2022)

A number of recent experiments report the low-temperature thermopower α and specific heat coefficients $\gamma = C_V/T$ of strongly correlated electron systems. Describing the charge and heat transport in a thermoelectric by transport equations, and assuming that the charge current and the heat current densities are proportional to the number density of the charge carriers, we obtain a simple mean-field relationship between α and the entropy density $\mathcal{S}$ of the charge carriers. We discuss corrections to this mean-field formula and use results obtained for the periodic Anderson and the Falicov-Kimball models to explain the concentration (chemical pressure) and temperature dependence of $\alpha/\gamma T$ in $EuCu_2(Ge_{1-x}Si_x)_2$, $CePt_{1-x}Ni_x$, and $YbIn_{1-x}Ag_xCu_4$ intermetallic compounds. We also show, using the 'poor man's mapping' which approximates the periodic Anderson lattice by the single impurity Anderson model, that the seemingly complicated behavior of $\alpha(T)$ can be explained in simple terms and that the temperature dependence of $\alpha(T)$ at each doping level is consistent with the magnetic character of $4f$ ions.

PACS numbers: 75.30.Mb, 72.15.Jf, 62.50.+p, 75.30.Kz,

I. INTRODUCTION

Several recent papers[1,2,3] report on a correlation between the low-temperature thermopower α and the specific heat coefficient $\gamma = C_V/T$ for heavy Fermions and valence fluctuating compounds with Ce, Eu, Yb and U ions. The data show that the zero-temperature limit of the ratio $\alpha(T)/C_V(T) = \alpha/\gamma T$ in most systems is about the same, although the absolute values of γ and α/T vary by orders of magnitude[1,2,3,4,5,6,7,8,9,10,11]. At the moment it is not clear if the deviations from universality arise because of insufficient accuracy of the data, or because the 'universal law' is only approximately valid. The difficulty is that neither $\alpha(T)$ nor $C_V(T)$ are linear in the lowest available temperature intervals and to obtain the linear coefficients one has to estimate the functional form of $\alpha(T)$ and $C_V(T)$ before taking the zero-temperature limit. The temperature dependences of $\alpha(T)$ and $C_V(T)$ in various systems might have a different physical origin, and comparing the data on $\alpha(T)/\gamma T$ without a detailed knowledge of the underlying dynamics might lead to erroneous conclusions. Furthermore, the definition of the 'zero-temperature limit' can differ considerably for systems with vastly different characteristic temperatures and at present it is not clear what the error bars are for the $\alpha/\gamma T$ data. We believe, the universality of the $\alpha/\gamma T$ ratio could be tested most directly by performing a pressure experiment which transforms Ce- or Eu-based heavy Fermion materials into valence fluctuators, and Yb-based valence fluctuators into heavy Fermion materials. Pressure can not only change the characteristic temperature of a given compound by several orders of magnitude[12,13] and, with that, change the nature of the ground state, but it has a dramatic effect on the overall shape of the thermopower. Although the low-temperature pressure experiments are less accurate than the ambient pressure ones, the evolution of $\alpha(T)$ or $C_V(T)$ with pressure could be followed and the universality of $\alpha/\gamma T$ studied in a systematic way. Experiments which provide the low-temperature thermopower and the specific heat on the same sample at various pressures are yet to be performed but some data are available on the doping dependence (chemical pressure) of α and γ. For example, doping alters α and γ of $EuCu_2(Ge_{1-x}Si_x)_2$, $CePt_{1-x}Ni_x$ and $YbIn_{1-x}Ag_xCu_4$ intermetallics by more than one order of magnitude[4,5,6,7,8,9]. while barely affecting the low-temperature ratio $\alpha/\gamma T$. We explain this behavior as a chemical pressure effect.

A simple relation between α and γT is obtained for a free electron gas and for non-interacting electrons on a lattice. The solution of the Boltzmann equation gives, under fairly general conditions, the result[14,15] $\alpha(T) \simeq \mathcal{S}(T)/ne = C_V(T)/ne$, where $\mathcal{S}$ is the entropy density, n the number density of the charge carriers and the second equality holds because the specific heat is linear with T at low T. But non-interacting electrons fail to describe the properties of the compounds mentioned above and the question arises to what extent does the 'universal relation' between α and $\mathcal{S}$ (or C_V) hold for strongly correlated electrons?

On a macroscopic level, an analysis of the charge and heat transport of a thermoelectric in terms of transport equations yields the same relationship between α and $\mathcal{S}$ as the free electron model. This derivation assumes that under isothermal conditions the expectation value of the charge current density is proportional to the expectation value of the heat current density, and we expect it to be valid for Fermi liquids (FL); of course, this is neglecting

other sources of heat transport, such as phonon contributions (but those do not enter into isothermal heat transport unless there are phonon drag effects). In the case of the non-FL compounds, where $C_V(T)/T$ and $\alpha(T)/T$ are temperature-dependent, instead of $\alpha/T\gamma$ one should consider the ratio $\alpha/\mathcal{S}$.

The zero-temperature $\alpha/\gamma T$-ratio has been discussed recently by Miyake and Kohno[16]. They calculate the dynamical conductivity of the periodic Anderson model in the quasiparticle (QP) approximation and obtain the Seebeck coefficient from the canonical formula which expresses $\alpha(T)$ as the ratio of two transport integrals[17]. The universal FL behavior is derived by assuming that in addition to the renormalization effects due to the Coulomb interaction between *f*-electrons, the charge and heat transport are affected by the scattering of quasiparticles off residual impurities. This scattering dominates the transport relaxation time and gives rise to a finite residual resistivity ρ_0. In the dilute limit, the impurity concentration drops out of the ratio of transport integrals and does not appear in the expression for the Seebeck coefficient.

The exact many-body transport coefficients of the periodic spin-1/2 Anderson model have recently been obtained at finite temperatures by Grenzebach et al.[18] using the dynamical mean field theory (DMFT) which maps the lattice problem onto an auxiliary single impurity model with a self consistency condition. The electron relaxation is solely due to the Coulomb repulsion between *f*-electrons and the model describes both heavy Fermions and valence fluctuators with vanishing ρ_0. The solution of the auxiliary impurity problem is obtained by the numerical renormalization group (NRG) method, which provides accurate results for the static properties at arbitrary temperature and for the dynamical properties above the FL regime. However, the zero-temperature limit of the transport relaxation time is difficult to obtain by the DMFT+NRG method (due to numerical issues associated with the self-consistency), and the validity of the FL laws for the transport coefficients of strongly correlated electrons has not been clearly established.

In this contribution, we discuss the zero-temperature $\alpha/\gamma T$-ratio for the periodic Anderson model and the Falicov-Kimball model, which describe heavy Fermions and valence fluctuators with crystal field (CF) split 4*f*-states. In this limit the excited CF states are not occupied and we calculate the slope of $\alpha(T)$ using the DMFT solution of an effective $\mathcal{M}$-fold degenerate model. The result agrees with that of Miyake and Kohno[16] even though we consider a periodic model with vanishing ρ_0 and have a positive coefficient for the T^2 term of the electrical resistance. We also analyze the influence of CF splittings on the thermopower of the Anderson model above the FL regime. At present, the dynamical properties of such a model cannot be obtained by the exact DMFT mapping and we find the solution using an approximate 'poor man's mapping'. That is, we assume that the conduction electrons scatter incoherently off the 4*f*-ions, relate the transport relaxation time to the single-ion T-matrix, and solve the scattering problem by the non-crossing approximation (NCA), which can properly treat the highly asymmetric limit of the Anderson model and infinite Coulomb repulsion. The results obtained in such a way explain the concentration (chemical pressure) dependence of $\lim_{T\to 0}\alpha/\gamma T$ and the evolution of $\alpha(T)$ in $EuCu_2(Ge_{1-x}Si_x)_2$[3,4,5] $CePt_{1-x}Ni_x$[6], and $YbIn_{1-x}Ag_xCu_4$[8,9,19,20]. The thermoelectric properties of these systems exhibit all the typical features observed in heavy Fermions and valence fluctuators[21,22]. Our calculations show that the temperature dependence of $\alpha(T)$ at each doping level is consistent with the character of the ground state inferred from the initial thermopower slope.

The rest of this contribution is organized as follows. In Section II, we introduce the macroscopic transport equations, discuss the Seebeck and Peltier experiments, and find the relationship between the thermopower and the entropy. In Section III.1 we calculate the Seebeck coefficient of the periodic Anderson model in the FL regime using the DMFT mapping. In Section III.2 we calculate the finite-temperature behavior using the 'poor man's mapping'. In Section III.3 we discuss the thermoelectric properties of the Falicov-Kimball model using the DMFT approach. In Section IV, we use these results to discuss the experimental data on the intermetallic compounds mentioned above. Our conclusions are presented in Section V.

II. TRANSPORT EQUATIONS

We consider the macroscopic charge and energy currents which are given by the statistical averages $\mathbf{J} = \mathrm{Tr}\{\rho_\phi \hat{\mathbf{j}}\}$ and $\mathbf{J}_E^\phi = \mathrm{Tr}\{\rho_\phi \hat{\mathbf{j}}_E^\phi\}$, where ρ_ϕ is the density matrix, $\hat{\mathbf{j}}$ the charge current density and $\hat{\mathbf{j}}_E^\phi$ the energy current density operators for a system of charged particles in the presence of an external scalar potential ϕ. These operators are are obtained by commuting the Hamiltonian with the charge and energy polarization operators[17] respectively, which are chosen in such a way that the macroscopic currents satisfy the appropriate continuity equations[23]. Assuming that the external potential couples to the charge density, a direct calculation shows[24] that $\hat{\mathbf{j}}$ is field independent and $\hat{\mathbf{j}}_E^\phi = \hat{\mathbf{j}}_E + \phi\hat{\mathbf{j}}$, where $\hat{\mathbf{j}}_E$ is the energy current density defined by the field-free Hamiltonian. The macroscopic energy current $\mathbf{J}_E = \mathrm{Tr}\{\rho_\phi \hat{\mathbf{j}}_E\}$ does not satisfy the continuity equation in the presence of the external potential but is easily calculated by a perturbative expansion. The gradient expansion of ρ_ϕ produces linearized equations[25], $\mathbf{J} = L_{11}\mathbf{x}_c + L_{12}\mathbf{x}_E$ and $\mathbf{J}_E = \mathbf{J}_{E_\phi} - \phi\mathbf{J} = L_{21}\mathbf{x}_c + L_{22}\mathbf{x}_E$, where the generalized forces are given by $\mathbf{x}_c = -\nabla\phi - T\nabla(\mu/eT)$ and $\mathbf{x}_E = -\nabla T/T$, μ is the chemical potential and $e = -|e|$ the electron charge. The (linear-response) expansion coefficients are given by the

correlation functions,

$$L_{ij}^{\alpha\beta} = \lim_{s\to 0} \frac{1}{V} \int_0^\infty dt e^{-st} \int_0^\beta d\beta \langle \hat{\mathbf{j}}_i^\alpha(-t-i\beta)\hat{\mathbf{j}}_j^\beta(0)\rangle_0, \quad (1)$$

where $\langle \hat{\mathbf{j}}_i^\alpha \hat{\mathbf{j}}_j^\beta \rangle_0 = \mathrm{Tr}\{\rho\, \hat{\mathbf{j}}_i^\alpha \hat{\mathbf{j}}_j^\beta\}$ denotes the statistical average in the absence of the external potential and $\hat{\mathbf{j}}_1^\alpha$ and $\hat{\mathbf{j}}_2^\beta$ denote the $q = 0$ Fourier components of $\hat{\mathbf{j}}^\alpha(x)$ and $\hat{\mathbf{j}}_E^\beta(x)$, respectively ($\alpha$, β denote the coordinate axes). In what follows, we assume a homogenous and isotropic conductor in the absence of a magnetic field and consider only a single Cartesian component of $\hat{\mathbf{j}}$ and $\hat{\mathbf{j}}_E$ (this is appropriate for cubic systems).

Thermoelectric effects are usually described in terms of the heat current, hence we transform the linearized equations from $\mathbf{J}$ and $\mathbf{J}_E$ to $\mathbf{J}$ and $\mathbf{J}_Q = \mathbf{J}_E - (\mu/e)\mathbf{J}$ to yield[17,27]

$$\mathbf{J} = -\sigma\nabla\phi - \sigma\alpha\nabla T, \quad (2)$$

$$\mathbf{J}_Q = \alpha T\mathbf{J} - \kappa\nabla T, \quad (3)$$

where $\sigma = L_{11}$, $\alpha T = (L_{12}/L_{11} - \mu/e)$, and $\kappa T = (L_{22} - L_{12}^2/L_{11})$. A simple analysis shows that $\sigma(T)$, $\alpha(T)$, and $\kappa(T)$ are the isothermal electrical conductivity, the Seebeck coefficient and the thermal conductivity, respectively[26,27]. The Onsager relation[28] gives $\alpha T = \Pi$, where Π is the Peltier coefficient.

The stationary temperature distribution across the sample is obtained from the total energy current in a field $\mathbf{J}_E^\phi = \mathbf{J}_Q + (\phi + \mu/e)\mathbf{J}$ which satisfies the energy continuity equation[23] $\mathrm{div}\mathbf{J}_E^\phi = 0$ and leads to the Domenicali equation[26],

$$\dot{E}_\phi = \mathrm{div}(\kappa\nabla T) + \frac{\mathbf{J}^2}{\sigma} - T\mathbf{J}\cdot\nabla\alpha = 0. \quad (4)$$

The Joule term (J^2/σ) in Eq. (4) is crucial for the total energy balance and for establishing the correct steady-state temperature distribution.

The solution of Eqs. (2)–(4), with appropriate boundary conditions, completely specifies the thermoelectric response of the system. The above procedure connects the theoretical model of a given material with the phenomenological transport coefficients and could be used, in principle, to explain the experimentally established relationship between the thermopower and the specific heat. However, for general many body systems such a program cannot be completed and, at first sight, it is not obvious that the transport coefficients, which depend on the dynamical properties of the system, are simply related to the thermodynamic quantities, which depend only on the static properties[15]. For example, the heat current considered in this many-body theory is just the electronic contribution to the heat transport, hence we only expect it to relate to the appropriate electronic contributions to the entropy. On a macroscopic level, the relationship between α and $\mathcal{S}$ can be obtained by solving Eqs. (2) and (3) once with the boundary conditions corresponding to the measurement of the Seebeck coefficient and once with those appropriate for the measurement of the Peltier coefficient.

In the Seebeck setup (an open circuit without net charge current), the thermoelectric voltage is induced by the heat flow due to the temperature gradient. The Seebeck voltage appears because the charged particles diffuse from the hot to the cold end and the imbalance of charge gives rise to a potential gradient across the sample. The Seebeck coefficient is obtained from the ratio $\Delta V/\Delta T$, where $\Delta V = -\int_0^a dx\ \nabla\phi(\mathbf{x})$ is the voltage change and $\Delta T = \int_0^a dx\ \nabla T(\mathbf{x})$ the temperature drop between the end-points of a sample of length a. For constant $\alpha(x)$, Eq. (2) gives $\Delta V = \alpha\Delta T$. In a stationary state, a quasiparticle picture says that the electrical energy required to transfer n electrons from the hot end to the cold end against the voltage ΔV is balanced by the change in thermal energy (that is, the heat). Neglecting the shift of the quantum states due to the external potential, we approximate $ne\Delta V \simeq \mathcal{S}_n\Delta T$, where n is the particle density and $\mathcal{S}_n$ the entropy density of the charge carriers. This gives the approximate relationship between the Seebeck coefficient and the entropy as

$$\alpha(T) = \frac{\mathcal{S}_n(T)}{en}. \quad (5)$$

In the Peltier setup, a constant electrical current passing through a junction of two different thermoelectrics gives rise to an additional heat current emanating at the interface of the junction. The Peltier heat appears because the excitation spectra on the two sides of the interface are different, so that the charge transfer produces an entropy change. (The entropy of n particles is determined by the structure of the energy levels over which the current carriers are distributed.) In a stationary state, the normal component of currents and temperature are continuous across the junction but ∇T and the transport coefficients are discontinuous. Integrating Eq. (4) over a thin volume element containing the interface gives[27],

$$-\kappa_s\nabla T|_s - (-\kappa_l\nabla T|_l) = -\mathbf{J}T(\alpha_s - \alpha_l), \quad (6)$$

where we used Gauss theorem and neglected the Joule heat. κ_s, $\nabla T|_s$, α_s and κ_l, $\nabla T|_l$, α_l denote the thermal conductivity, temperature gradient and the Seebeck coefficient of the 'sample' and 'leads' in the vicinity of the interface. Eq. (6) shows that the heat brought to and taken from the surface by the thermal conductivity differs by $\Pi_{sl}\mathbf{J}$, where Π_{sl} is the relative Peltier coefficient of the two materials, $\Pi_{sl} = T[\alpha_s(T) - \alpha_l(T)]$. In other words, the junction generates an additional heat current $\Pi_{sl}\mathbf{J}$ which maintains the stationary state by absorbing (or releasing) heat from the environment. Depending on the sign of $\mathbf{J}$, the Peltier heat is either absorbed or released, i.e., the entropy change due to the Peltier effect is reversible.

Under stationary isothermal conditions, and for currents flowing in the x-direction, Onsager's relation gives

$$\alpha(T) = \frac{J_Q}{TJ}, \quad (7)$$

where J_Q is the Peltier heat current. Neglecting the Joule heat and assuming that the stationary state is maintained by a heat source at one end and a sink at the other end of the sample, we can simplify Eq. (7) using div $\mathbf{J} = 0$ and div $\mathbf{J}_Q = 0$. For such divergence-free currents, we assume that the charge and heat flow uniformly with a drift velocity $\mathbf{v}$ and write $\mathbf{J} = ne\mathbf{v}$ and $\mathbf{J}_Q = Q_n\mathbf{v}$, where $Q_n = \alpha Tne$ is the Peltier heat generated at the lead-sample interface and transported by the current in the lead to the sink. Defining the reversible thermoelectric entropy density as $\mathcal{S}_n(T) = Q_n/T$, we reduce Eq. (7) to Eq. (5). Finally, multiplying both sides of Eq. (5) by $N_A e$, where N_A is Avogadro's constant, and dividing by the molar entropy $\mathcal{S}_N(T) = \mathcal{S}_n(T)\Omega$, where Ω is the molar volume of the material under study, we obtain a dimensionless parameter

$$q = N_A \frac{e\alpha(T)}{\mathcal{S}_N(T)} = (\frac{N}{N_A})^{-1}, \tag{8}$$

which characterizes the thermoelectric material in terms of an effective charge carrier concentration per formula unit (or the Fermi volume V_F of the charge carriers). For Fermi liquids, $\mathcal{S}(T) = \gamma T$ at low temperature and we obtain

$$q = N_A e \frac{\alpha(T)}{\gamma T}, \tag{9}$$

which is the quantity defined by Behnia, *et al.*[2]. Throughout this paper, α is expressed in [μV/K], C_V and $\mathcal{S}$ in [J/(K mol)], and the Faraday number is $N_A e = 9.6 \times 10^4$C/mol.

Before proceeding, we should comment on the validity of the above approximations. As mentioned already, the entropy of the charge carriers in the steady state which characterizes the Seebeck setup is not the same as the equilibrium entropy, because the steady-state potential is different at the hot and the cold end. As regards the Peltier setup, the average value of the current density operator is not simply proportional to the particle density, and the definition used in Eq. (8) neglects all the operator products which lead to higher-order powers in the particle density. This amounts to describing the low-energy excitations of the system by quasiparticles and approximating the many-body interactions by self-consistent fields.

Furthermore, we should take into account that the entropy $\mathcal{S}_n$ in Eq. (5) or $\mathcal{S}_N$ in Eq. (8) is not the full entropy $\mathcal{S}$ of the system, but only the entropy of the charge carriers appearing in the transport equations. For example, the total entropy $\mathcal{S}$ might have contributions $\mathcal{S}_M$ coming from additional degrees of freedom, like localized paramagnetic states, magnons or phonons, which do not participate in the charge transport and are only weakly coupled to the charge carrying modes. Assuming $\mathcal{S} = \mathcal{S}_N + \mathcal{S}_M$ but neglecting the contribution of these additional degrees of freedom to the charge transport, we get the experimentally determined quantity

$$\tilde{q} = N_A \frac{e\alpha(T)}{\mathcal{S}(T)} = \frac{N_A}{N} \frac{1}{1 + \mathcal{S}_M(T)/\mathcal{S}_N(T)}, \tag{10}$$

which could be much reduced with respect to $q = N_A/N$ given by Eq. (8). The experimental values $\tilde{q}$ depend not only on the concentration of carriers but also on temperature, and to get the universal ratio one might need a very low temperature, where $\mathcal{S}_M \ll \mathcal{S}_N$. This behavior is similar to deviations of the Wiedemann-Franz law from ideal metallic behavior whenever the phonon contribution to the heat current is substantial—in order for Wiedemann-Franz to hold, we need to have the phonon contribution to the thermal conductivity be much smaller than the electronic contribution.

The Seebeck coefficient appearing in Eqs. (5)—(10) should also be treated with care. If there are several conductivity channels, the total thermopower is a weighted sum of all the components $\sigma\alpha = \sum_j \sigma_j\alpha_j$, where $\sigma = \sum_j \sigma_j$, and there might be some cancellations in the thermopower sum. But $\mathcal{S}$ has different vertex corrections and the specific heat is not affected by these cancellations. Similarly, if there are several scattering channels for conduction electrons, vertex corrections give rise to interferences which affect the thermopower (like in the Friedel phase shift formula[29]). Even if we neglect interference effects and use the Nordheim-Gorter rule[30] ($\rho\alpha = \sum_j \rho_j\alpha_j$, where $\rho = \sum_j \rho_j$ and ρ_j and α_j are the resistivity and thermopower due to the j-th scattering channel), the α_j-terms in the weighted sum might have different signs and cancel. Thus, unless one of the channels dominates, $\tilde{q}$ is non-universal and temperature-dependent, and the interpretation becomes difficult. We also remark that the heat conductivity of magnons and phonons can give rise to phonon-drag and spin-drag contributions to $\alpha(T)$, which are not included in Eqs. (8) or (10). However, at low temperatures, those contributions are expected to be small.

For systems with a non-linear $C_V(T)$, like Yb and Ce compounds close to a quantum critical point[10,11], the experimental data cannot be analyzed in terms of Eq. (9), even at low temperatures, but one could use Eq. (8) instead. However, if the single-particle states are not well defined and thermal transport is due to collective excitations rather than quasiparticles, like in a Luttinger liquid[31], the significance of N/N_A as the number of the current carrying particles per formula unit, is no longer obvious.

III. MODEL CALCULATION OF THE SEEBECK COEFFICIENT

Considering the limitations and uncertainties mentioned above, it is somewhat surprising that in many correlated systems the low-temperature ratio of the thermopower and the specific heat comes quite close to the universal value given by Eq. (9). In what follows, we show

that the universal law of Sakurai[1] and Behnia[2] holds for the periodic Anderson model with on-site hybridization and for the Falicov-Kimball model. We also show that these models explain the full temperature dependence of the Seebeck coefficient observed in the intermetallic compounds with Ce, Eu and Yb ions. The charge current operator in both models is

$$\hat{\mathbf{j}} = e\sum_{\mathbf{k}\sigma} \mathbf{v}_{\mathbf{k}} c^{\dagger}_{\mathbf{k}\sigma} c_{\mathbf{k}\sigma}, \tag{11}$$

where σ labels the symmetry channels (irreducible representations to which the conduction electrons belong) and $\mathbf{v}_{\mathbf{k}} = \nabla\epsilon(\mathbf{k})$ is the velocity of unperturbed conduction electrons. Calculating the heat current density operators for a constant hybridization in $\mathbf{k}$-space we verify explicitly the Jonson-Mahan theorem[32] and find for each symmetry channel the static conductivity satisfies

$$\sigma(T) = \int d\omega \left(-\frac{df}{d\omega}\right) \Lambda(\omega, T) \tag{12}$$

and the thermopower satisfies

$$\alpha(T) = -\frac{1}{|e|T} \frac{\int d\omega \left(-\frac{df}{d\omega}\right) \omega\Lambda(\omega, T)}{\int d\omega \left(-\frac{df}{d\omega}\right) \Lambda(\omega, T)}. \tag{13}$$

The excitation energy ω is measured with respect to μ, $f(\omega) = 1/[1 + \exp(\beta\omega)]$ is the Fermi-Dirac distribution function and $\Lambda(\omega, T)$ is the charge current - charge current correlation function[17] (our result differs from Mahan's by an additional factor of e^2 from the charge current operators). In the low-temperature FL limit, the charge current - charge current correlation function is approximately found from the reducible vertex function by

$$\Lambda(\omega, T) = \frac{e^2}{V} \sum_{\mathbf{k}\sigma} \mathbf{v}_{\mathbf{k}}{}^2 G^{\sigma}_c(\mathbf{k}, \omega + i\delta) G^{\sigma}_c(\mathbf{k}, \omega - i\delta) \times \gamma^{\sigma}(\mathbf{k}, \omega + i\delta, \omega - i\delta). \tag{14}$$

Here $G^{\sigma}_c(\mathbf{k}, \omega \pm i\delta)$ are the momentum and energy-dependent retarded and advanced Green's function of the conduction electrons and $\gamma^{\sigma}(\mathbf{k}, \omega + i\delta, \omega - i\delta)$ is the analytic continuation from the imaginary axis into the complex plane of the (reducible) scalar vertex function $\gamma^{\sigma}(\mathbf{k}, i\omega_n)$, which is defined by the diagrammatic expansion of the current-current correlation function[17]. The details of the calculations are model-dependent and, in what follows, we consider separately the periodic Anderson model and the Falicov-Kimball model. One can also determine the charge current - charge current correlation function exactly within DMFT, where the vertex corrections vanish, and

$$\Lambda(\omega, T) = \frac{e^2}{V} \sum_{\mathbf{k}\sigma} \mathbf{v}^2_{\mathbf{k}} \left[\mathrm{Im} G^{\sigma}_c(\mathbf{k}, \omega + i\delta)\right]^2. \tag{15}$$

This form is particularly useful if $G^{\sigma}_c(\mathbf{k}, \omega + i\delta)$ is known for all $\mathbf{k}$ and ω points; we use it for evaluating the Falicov-Kimball model[33,34], since it does not have FL behavior in general.

1. *Periodic Anderson model - the low-temperature DMFT solution*

The periodic Anderson model is defined by the Hamiltonian

$$H_A = H_c + H_f + H_{cf}, \tag{16}$$

where H_c describes the conduction electrons hopping on the lattice, H_f describes the $4f$ states localized at each lattice site, and H_{cf} describes the hybridization of electrons between $4f$ and conduction states. The total number of conduction electrons and *f*-electrons per site is n_c and n_f, respectively. We consider the model with an infinitely strong Coulomb repulsion between *f*-electrons (or *f*-holes) which does not allow two *f*-electrons to occupy the same lattice site. That is, we strictly enforce the constraint $n_f \leq 1$ (or $n^h_f \leq 1$), and also choose $n_c \leq 1$. The total number of electrons $n = n_c + n_f$ is conserved. The unrenormalized density of states (DOS) of the conduction electrons in each channel is $\mathcal{N}^0_c(\epsilon) = \sum_{\mathbf{k}} \delta(\epsilon - \epsilon_{\mathbf{k}})$, where $\epsilon_{\mathbf{k}}$ is the conduction-electron dispersion. We assume $\mathcal{N}^0_c(\epsilon)$ to be a symmetric, slowly varying function of half-width D, which is the same in all channels, and measure all the energies, except ω, with respect to its center. In the case of heavy Fermions and valence fluctuators with Ce ions, the non-magnetic state is represented by an empty *f*-shell and the magnetic state by the CF levels. We consider $M - 1$ excited CF levels separated from the CF ground state by energies $\Delta_i \ll |E_f|$, where $i = 1, \ldots, M - 1$. Each CF state belongs to a given irreducible representation of the point group Γ_i and its degeneracy is $\mathcal{L}_i$, such that $\mathcal{L} = \sum_i \mathcal{L}_i$. The spectral functions of the unrenormalized *f*-states are given by a set of delta functions at E^0_f and $E^i_f = E^0_f + \Delta_i$. The mixing matrix element V_i connects the conduction and *f*- states belonging to the same irrep and, for simplicity, we consider the case $V_i = V$ for all channels, i. e. the hybridization is characterized by the parameter $\Gamma = \pi V^2 \mathcal{N}^0_c(0)$. The conduction and *f*-states have a common chemical potential μ. The properties of the model depend in an essential way on the coupling constant $g = \Gamma/\pi|E_f - \mu|$, where $E_f = \sum_i \mathcal{L}_i E^i_f/\mathcal{L}$ and on the CF splittings. For $\mathcal{L} > 2$ and strong correlation between the *f*-electrons, the condition $n_f \leq 1$ makes the model extremely asymmetric; $n_f \simeq 1$ can only be reached for very small g. In such a model, an increase in g gives rise to a monotonic reduction of n_f, which assumes a characteristic value at each fixed point. An application of pressure or chemical pressure (doping) to Ce systems is modeled by an increase of the bare coupling g, which decreases n_f. In the case of Europium the non-magnetic $4f^{\,6}$ state is a Hund's singlet and the magnetic state is a degenerate $4f^{\,7}$ Hund's octet with full rotational invariance. The Eu ion fluctuates between the two configurations by exchanging a single electron with the conduction band and we model the pressure effects in the same way as for Ce. In the case of Ytterbium, the non-magnetic state is the full-shell $4f^{\,14}$ configuration and the magnetic one is the

$4f^{13}$ configuration, which can be split by the CF. Here, pressure or chemical pressure reduce g and enhance the number of f-holes.

We first consider the CF and spin degenerate case ($\Delta_i = 0$ for all $\mathcal{L}$ f-states) and treat the correlations by the DMFT which is exact in the limit of infinite dimensions[35,36,37]. To simplify the notation we drop the spin-label in this subsection. Using the equations of motion for the imaginary time Green's functions, making the Fourier transform to Matsubara frequencies and analytically continuing into the complex energy plane, we obtain the Dyson equations for the c- and f-electrons Green's functions,

$$G_c(\mathbf{k},z) = \frac{z-(E_f-\mu)-\Sigma_f(\mathbf{k},z)}{[z-(\epsilon_{\mathbf{k}}-\mu)][z-(E_f-\mu)-\Sigma_f(\mathbf{k},z)]-V^2}, \tag{17}$$

and

$$G_f(\mathbf{k},z) = \frac{z-(\epsilon_{\mathbf{k}}-\mu)}{[z-(\epsilon_{\mathbf{k}}-\mu)][z-(E_f-\mu)-\Sigma_f(\mathbf{k},z)]-V^2}, \tag{18}$$

where z satisfies $z=\omega+i\delta$ and $\Sigma_f(k,z)$ is the f-electron self energy (the self energy and Green's functions are identical for each of the $\mathcal{L}$ different f-states). The retarded (advanced) Green's functions are defined by the above expressions for z in the upper (lower) part of the complex plane and are denoted on the real axis by $\omega^{\pm}=\lim_{\delta\to 0}(\omega\pm i\delta)$. The self energy of the conduction electrons is

$$\Sigma_c(\mathbf{k},z) = \frac{V^2}{z-(E_f-\mu)-\Sigma_f(\mathbf{k},z)}. \tag{19}$$

In DMFT, the self-energies are momentum independent: $\Sigma_f(\mathbf{k},z)=\Sigma_f(z)$ and $\Sigma_c(\mathbf{k},z)=\Sigma_c(z)$, and the model is solved by mapping the local Green's function, $G_f(z)=\sum_{\mathbf{k}} G_f(\mathbf{k},z)$, onto the Green's function of an auxiliary single impurity Anderson model,

$$G_f(z) = \frac{1}{z-(E_f-\mu)-\Delta(z)-\Sigma_f(z)}, \tag{20}$$

where $\Delta(z)$ is determined by the requirement that Eqs. (17) - (20) are self-consistently solved and that $\sum_{\mathbf{k}} G_f(\mathbf{k},z)$ is equal to $G_f(z)$ in Eq. (20). The irreducible self energy of the lattice and the impurity are given by the same functional, $\Sigma_f[\sum_{\mathbf{k}} G_f(\mathbf{k},\omega)] = \Sigma_f[G_f(\omega)]$, and the self-consistency requires that the auxiliary spectral function, $A(\omega)=-Im\ G_f(\omega^+)/\pi$ coincides with the local f-DOS of the lattice, $\mathcal{N}_f(\omega)=\sum_{\mathbf{k}} A_f(\mathbf{k},\omega)$, where

$$A_f(\mathbf{k},\omega) = -\frac{1}{\pi} Im\ G_f(\mathbf{k},\omega^+). \tag{21}$$

The impurity model generated by the DMFT describes a single f-electron distributed over $\mathcal{L}$-fold degenerate spin or CF states and the double occupancy of these states is explicitly forbidden, $n_f \le 1$. The energy of the effective impurity f-state is E_f and the coupling to the auxiliary conduction band is described the hybridization function $\Delta(\omega^+)$. Since n_f is the same on the impurity and on the lattice, for large $\mathcal{L}$ the impurity model is highly asymmetric. For $\omega \simeq 0$, we assume that the ω-dependence of $\Delta(\omega)$ is much slower than of $Im\ \Sigma_f(\omega^+,T)$ and approximate, $\Delta(\omega)\simeq\Delta(0)=i\Delta_0$. The positive-definiteness of $\mathcal{N}_f(\omega)$ requires $\Delta_0<0$.

The DMFT simplifies the calculation of the current-current correlation functions and the transport coefficients. In infinite dimensions the vertex corrections to $\Lambda(\omega)$ vanish[38], so that $\gamma(\mathbf{k},\omega)=1$, and once the self-consistency condition is satisfied, the transport properties are determined by the self-energy of the impurity model. From the causality of the problem it follows that $Im\ \Sigma_f(\omega^+,T)$ is negative on the real ω-axis. At $T=0$, the imaginary part of the self energy of the auxiliary impurity model has a maximum at $\omega=0$, such that[40] $Im\ \Sigma_f(0)=0$, $Im\left[\partial\Sigma_f/\partial\omega\right]_{\omega=0^+}=0$, and $Im\left[\partial^2\Sigma_f/\partial\omega^2\right]_{\omega=0^+}<0$.

The charge-current correlation function [for the FL at low temperature where we use Eq. (14) instead of Eq. (15) since it is the dominant contribution when $T\to 0$] follows from the identity $G_c(\mathbf{k},\omega^+)G_c(\mathbf{k},\omega^-) = -A_c(\mathbf{k},\omega)/Im\ \Sigma_c(\omega^+,T)$, where

$$A_c(\mathbf{k},\omega) = -\frac{1}{\pi} Im\ G_c(\mathbf{k},\omega^+) \tag{22}$$

is the spectral function of conduction electrons. This gives

$$\Lambda(\omega,T) = \frac{-e^2}{V\ Im\Sigma_c(\omega^+,T)} \sum_{\mathbf{k}} {v_{\mathbf{k}}}^2 A_c(\mathbf{k},\omega), \tag{23}$$

and can be further simplified by taking into account that the factor $(-df/d\omega)$ restricts the transport integrals to the Fermi window, $|\omega|\le k_BT$. The main contribution to transport integrals comes from the $\mathbf{k}$-points in the vicinity of the renormalized Fermi surface (FS) and in this narrow region of $(\mathbf{k},\omega)$–space we approximate $v_{\mathbf{k}}^2$ by its FS average, $\langle v_{k_F}^2\rangle$. This gives the usual result,

$$\Lambda(\omega,T) = e^2\langle {v_{k_F}}^2\rangle \mathcal{N}_c(\omega)\ \tau(\omega,T), \tag{24}$$

where the renormalized c-DOS is defined by

$$\mathcal{N}_c(\omega) = \sum_{\mathbf{k}} A_c(\epsilon_{\mathbf{k}},\omega), \tag{25}$$

and the transport relaxation time is

$$\tau(\omega,T) = \frac{1}{-Im\ \Sigma_c(\omega^+,T)}. \tag{26}$$

Note, the approximate FL charge-current correlation function, given by Eq. (24), coincides with the exact DMFT result[33,34] only in the limit $T,\omega\to 0$ (the DMFT result has another term, which can be neglected as $T\to 0$, but is important at finite T or for non FL systems).

It is a challenge to determine the conductivity and Seebeck coefficient at low temperature for a FL described by a transport relaxation time given in Eq. (26), because the rhs diverges when ω and T both equal zero. Since $Im\Sigma_f(\omega^+,T) \approx -|c|(\omega^2+\pi^2T^2/2)$ for a FL, we see that the proper way to take the limit of $T \to 0$ is to first consider the limit $\omega \to 0$ at finite T and then examine what happens as $T \to 0$. Doing so, will allow for a proper calculation of the Seebeck coefficient, which is finite, even though it is determined as the ratio of two integrals, each becoming infinite as $T \to 0$.

With these ideas in mind, we substitute Eq. (19) for $Im\ \Sigma_c(\omega^+,T)$ to give

$$\tau(\omega,T) \simeq \lim_{\delta\to 0} \frac{[\omega-\tilde{\epsilon}_f(\omega,T)+\mu]^2+[Im\ \Sigma_f(\omega^+,T)]^2}{\delta - Im\ \Sigma_f(\omega^+,T)V^2}, \tag{27}$$

where $\tilde{\epsilon}_f(\omega,T) = E_f + Re\ \Sigma_f(\omega^+,T)$ and the limit is taken in such a way that $\omega \to 0$ before $\delta \to 0$ (i. e., we take $\omega \to 0$ before $T \to 0$). At low temperature, we do not expect $-\tilde{\epsilon}_f(\omega,T)+\mu$ to vanish, because it vanishes for the single-band model at half filling, and we have a multiband model far from half filling. In the following, we assume that $-\tilde{\epsilon}_f(\omega,T)+\mu$ is much larger (in absolute magnitude) than ω or T in the low-frequency and low-temperature regime. For a given value of V, E_f and n, we calculate $\Sigma_f(\omega)$, $\tilde{\epsilon}_f(\omega,T)$, $\mathcal{N}_f(\omega)$, $\mathcal{N}_c(\omega)$, n_f and n_c by the DMFT procedure and find the renormalized μ from the condition $n_f + n_c = n$.

The low-temperature Seebeck coefficient is obtained from Eqs. (13) and (24) by the Sommerfeld expansion. It is a weighted sum of the contribution of all the symmetry channels, which, all of them being equivalent, is equal to the single channel value. To lowest order:

$$\frac{\alpha(T)}{T} = -\frac{\pi^2}{3}\frac{k_B^2}{|e|}\left\{\frac{1}{\mathcal{N}_c(\omega)}\frac{\partial \mathcal{N}_c(\omega)}{\partial\omega} + \frac{1}{\tau(\omega)}\frac{\partial\tau(\omega)}{\partial\omega}\right\}_{\omega,T=0}. \tag{28}$$

The quantity $\lim_{T\to 0}\tau_0(T) = \lim_{T\to 0}[\lim_{\omega\to 0}\tau(\omega,T)]$ diverges but the expressions given by the ratio of two transport integrals, like the one in Eq. (13), or the logarithmic derivative in Eq. (28), remain finite as the temperature goes to zero. Using $Im\Sigma_f(\omega) \simeq \omega^2$ at $T=0$ we obtain from Eq. (27)

$$\frac{d}{d\omega}[\ln\tau(\omega)]\Big|_{\omega=0} \simeq 2\left[\frac{1-\frac{\partial\Sigma_f(\omega)}{\partial\omega}}{\mu-\tilde{\epsilon}_f(\omega)}\right]_{\omega=0}. \tag{29}$$

To find $\alpha(T)/T$ in Eq. (28) we have to estimate the renormalized position of the f-states and the renormalized DOS at $\omega, T = 0$.

The low-energy densities of states $\mathcal{N}_c(\omega)$ and $\mathcal{N}_f(\omega)$ are determined by the analytic properties of $A_c(\epsilon_{\mathbf{k}},\omega)$ and $A_f(\epsilon_{\mathbf{k}},\omega)$, considered as functions of the variable $\epsilon_{\mathbf{k}}$ and for fixed values of ω, $\tilde{\epsilon}_f$, V, and μ. Using the fact that $A_c(\epsilon_{\mathbf{k}},\omega)$ and $A_f(\epsilon_{\mathbf{k}},\omega)$ depend on $\mathbf{k}$ only through $\epsilon_{\mathbf{k}}$ [see Eqs. (17) and (18) and recall that Σ_f is independent of $\mathbf{k}$ in DMFT] we write

$$\mathcal{N}_f(\omega) = \int d\epsilon\ \mathcal{N}_c^0(\epsilon)A_f(\epsilon,\omega), \tag{30}$$

and

$$\mathcal{N}_c(\omega) = \int d\epsilon\ \mathcal{N}_c^0(\epsilon)A_c(\epsilon,\omega), \tag{31}$$

where $\mathcal{N}_c^0(\epsilon)$ is the unrenormalized density of states of the conduction electrons (recall D is the half bandwidth of the unrenormalized band). For small ω, the main contribution to $\mathcal{N}_f(\omega)$ and $\mathcal{N}_c(\omega)$ is coming from the domain of integration in which the spectral functions diverge (once again, for the FL at low T). The condition for the singular region is obtained from Eqs. (18) and (17) as

$$\omega - \epsilon_{\mathbf{k}} + \mu = \frac{V^2}{\omega - \tilde{\epsilon}_f(\omega)+\mu}. \tag{32}$$

A straightforward calculation gives on the critical surface

$$A_c(\epsilon,\omega) \simeq \delta\left(\omega - \epsilon + \mu - \frac{V^2}{\omega-\tilde{\epsilon}_f+\mu}\right) \tag{33}$$

and

$$A_f(\epsilon,\omega) \simeq \frac{\omega-\epsilon+\mu}{\omega-\tilde{\epsilon}_f+\mu}\delta\left(\omega-\epsilon+\mu-\frac{V^2}{\omega-\tilde{\epsilon}_f+\mu}\right), \tag{34}$$

where we used $Im\Sigma_f(\omega) \simeq \omega^2 \ll \delta$ and $\delta^2 \ll V^2/D^2$. Note, the prefactor of the δ-function in Eq. (34) is positive definite. Further note how the argument of the delta function is the same for both the conduction and the f-electrons. But because this argument has a complicated dependence on frequency, there are actually two roots to the equation where we set the argument equal to zero. These two roots comprise the two distinct quasiparticle bands, which are the physical elementary excitation bands and are derived in detail below.

The integrals in Eqs. (30) and (31) are now straightforward to calculate and give the zero-temperature results

$$\mathcal{N}_c(\omega) = \mathcal{N}_c^0\left(\omega+\mu-\frac{V^2}{\omega-\tilde{\epsilon}_f(\omega)+\mu}\right), \tag{35}$$

and

$$\mathcal{N}_f(0) = \frac{\mu-\langle\epsilon_{\mathbf{k}}\rangle_{FS}}{\mu-\tilde{\epsilon}_f(0)}\mathcal{N}_c(0) = \frac{\mu-\epsilon_{\mathbf{k_F}}}{\mu-\tilde{\epsilon}_f(0)}\mathcal{N}_c^0(\epsilon_{\mathbf{k}_F}). \tag{36}$$

To derive these results, we assumed that $\epsilon_{\mathbf{k}}$ varies slowly on the renormalized Fermi surface defined by $\mathbf{k}_F$ and replaced $\epsilon_{\mathbf{k}}$ in Eq. (32) by the FS average $\epsilon_{\mathbf{k}_F}$. Note, $\mathcal{N}_f(\omega)$ and $\mathcal{N}_c(\omega)$ are implicit functions of the degeneracy factor $\mathcal{L}$. The total c- and f-DOS are obtained by multiplying the above expressions by $\mathcal{L}$. The renormalized densities of states in Eqs. (35) and (36) and the general properties

of the self energy of the auxiliary single impurity Anderson model[40] are sufficient to obtain the FL properties of the periodic Anderson model.

In the limit $T, \omega^+ \to 0$, we make a Taylor series expansion of $\Sigma_f(\omega^+)$ truncated to linear order and approximate $\omega - [\tilde{\epsilon}_f(\omega) - \mu] \simeq (\omega - \tilde{\omega}_f) Z_f^{-1}$, where $\tilde{\omega}_f$ is the renormalized position of the f-level which is given by the solution of the equation $\tilde{\omega}_f = \tilde{\epsilon}_f(\tilde{\omega}_f) - \mu$ and $Z_f^{-1} = [1 - \partial \Sigma_f / \partial \omega]_{\tilde{\omega}=0}$. Using $\tilde{\omega}_f = [\tilde{\epsilon}_f(0) - \mu] Z_f$ in Eq. (32) gives the secular equation for the quasiparticle excitations close to the FS

$$(\omega - \epsilon_{\mathbf{k}} + \mu)(\omega - \tilde{\omega}_f) = \tilde{V}^2, \tag{37}$$

where $\mathbf{k}$ defines the propagation vector of the QP and $\tilde{V} = V\sqrt{Z_f}$ is the renormalized hybridization. The two solutions of Eq. (37) give the QP bands with energy $\omega = \Omega_{\mathbf{k}}^{\pm}$ and dispersion[40]

$$\Omega_{\mathbf{k}}^{\pm} = \frac{1}{2}\left[(\epsilon_{\mathbf{k}} - \mu - \tilde{\omega}_f) \pm \sqrt{(\epsilon_{\mathbf{k}} - \mu - \tilde{\omega}_f)^2 + 4\tilde{V}^2}\right] + \tilde{\omega}_f, \tag{38}$$

where $\Omega_{\mathbf{k}}^{+}$ and $\Omega_{\mathbf{k}}^{-}$ describe the two QP branches separated by the hybridization gap $\tilde{V}_f^2/D$. The upper (lower) QP band is very flat for $\mathbf{k}$ close to the center (close to the boundary) of the Brillouin zone (BZ). The hybridized FS is defined by the equation $\Omega_{\mathbf{k}}^{\pm} = 0$.

The precise values of the renormalized quantities $\mathbf{k}_F$, $\tilde{\epsilon}_f(0)$ and μ can only be obtained from the numerical DMFT solution but the approximate values can be inferred from the Luttinger theorem which requires that the Fermi volume of hybridized electrons is unchanged by the Coulomb interaction U. For Ce and Eu compounds the condition $U > D$ restricts the number of f-electrons at each site to $n_f < 1$. We assume $n \leq 2$ and describe the occupied states of the hybridized system by the lower QP branch, such that $\mu < 0$. Choosing, for simplicity, $\tilde{\omega}_f + \mu \simeq 0$ we obtain from Eq. (38) that $|\Omega_{\mathbf{k}}^{\pm} + \mu| > \tilde{V}^2/D$ everywhere in the BZ and that $\Omega_{\mathbf{k}}^{+} - \Omega_{\mathbf{k}}^{-} \simeq D[1 + 2(\tilde{V}/D)^2] \simeq D$ close to the boundary and the center of the BZ. For Ce and Eu systems with $n < 2$ the function $\Omega_{\mathbf{k}}^{-}$ changes sign at $\mathbf{k}_F$ which is not too far from the unrenormalized values, i.e., $\mathbf{k}_F$ is close to the zone boundary. For this wave-vector we approximate $\Omega_{\mathbf{k}_F}^{+} - \Omega_{\mathbf{k}_F}^{-} \simeq \epsilon_{\mathbf{k}_F} - \mu \simeq D$ and estimate $(\epsilon_{\mathbf{k}_F} - \mu)\mathcal{N}_c(0) \simeq n_c/\mathcal{L}$. For Yb compounds we restrict $n_f^h < 1$ and assume that the system is more than half-filled, such that $\mu > 0$. The lower QP branch is full and the upper branch is fractionally occupied. Choosing again $\tilde{\omega}_f + \mu \simeq 0$ we obtain from Eq. (38) that $\mathbf{k}_F$ is close to the center of the BZ, such that $\epsilon_{\mathbf{k}_F} - \mu \simeq -D$ and $(\epsilon_{\mathbf{k}_F} - \mu)\mathcal{N}_c(0) \simeq -n_c/\mathcal{L}$. This shows that

$$\mathcal{N}_f(0) = \pm \frac{n_c}{\mathcal{L}} \frac{Z_f}{\tilde{\omega}_f}, \tag{39}$$

where the upper sign applies to Ce and Eu compounds in which the renormalized f-level is above μ ($\tilde{\omega}_f > 0$) and the lower sign applies to Yb compounds in which the renormalized f-level is below μ ($\tilde{\omega}_f < 0$). The relationship between the low-energy scale $\tilde{\omega}_f$ and the specific heat coefficient of the periodic Anderson model $\gamma \simeq (\pi^2 k_B^2/3)\mathcal{L}\mathcal{N}_f(0) Z_f^{-1}$ is provided by Eq. (39) as $\tilde{\omega}_f = (\pi^2 k_B^2/3)(n_c/\gamma)$.

Eqs. (36) and (39) can now be used to eliminate $[\mu - \tilde{\epsilon}_f(\omega)]$ from Eq. (29) and write the logarithmic derivative of $\tau(\omega)$ as,

$$\frac{d}{d\omega}[\ln \tau(\omega)]\Big|_{\omega, T=0} \simeq \mp \frac{2\mathcal{L}\mathcal{N}_f(0) Z_f^{-1}}{n_c}, \tag{40}$$

where the upper (lower) sign is appropriate for Ce and Eu (Yb) systems. Using for $\mathcal{N}_c(\omega)$ the result in Eq. (35), we find for a slowly varying $\mathcal{N}_0(\omega)$,

$$\frac{d}{d\omega}[\ln \mathcal{N}_c(\omega)] \ll \frac{d}{d\omega}[\ln \tau(\omega)]\Big|_{\omega=0}, \tag{41}$$

such that the first term in Eq. (28) can be neglected, and obtain for the low-temperature Seebeck coefficient the FL law

$$\alpha(T) = \pm \frac{2\gamma T}{|e| n_c} = \frac{2\gamma T}{|e| n_c} \frac{\tilde{\omega}_f}{|\tilde{\omega}_f|}. \tag{42}$$

The initial thermopower slope is positive when the Kondo resonance is above μ, which corresponds to the intermetallic compounds with Ce and Eu ions. It is negative when the Kondo resonance is below μ, which corresponds to the intermetallics with Yb ions.

The above considerations apply to the systems which fluctuate between a non-magnetic and a $\mathcal{L}$-fold degenerate magnetic state, such as heavy Fermions with large Kondo scale and valence fluctuators. They should also apply to heavy Fermions with the CF splitting, because at low enough temperatures the excited CF states are unoccupied and the magnetic configuration is characterized by the degeneracy of the lowest CF state. Using Eq. (42) and the charge neutrality condition $n = n_f + n_c$ we find that the reduction of n_f by pressure or chemical pressure enhances slightly the ratio $q = \lim_{T \to 0} \alpha(T)/\gamma T$. However, these changes are small and we expect the q-ratio to be nearly constant for all strongly correlated metals described by the Anderson model away from electron-hole symmetry.

Note, we calculate the transport properties of strongly correlated systems following a completely different route than Miyake and Kohno[16], even though the QP dispersion is exactly the same. In Ref. 16, the QP bands are obtained for an effective model of hybridized Fermions with renormalized parameters which take into account the on-site correlation. However, doubly-occupied f-states are not explicitly excluded from the Hilbert space of the effective Hamiltonian and the number of f-electrons is restricted to $n_f \leq 1$ only on the average. In such a Fermionic model, the charge and heat current density operators in the QP representation are given by

quadratic forms which commute with the effective Hamiltonian. The Jonson-Mahan theorem applies and the low-temperature thermopower is obtained from the canonical expression in Eq. (28). The quasiparticle relaxation is due to scattering off external impurities, which give rise to a finite residual resistivity, and the logarithmic derivatives of the QP density of states and the transport relaxation time are of the same order of magnitude.

In our approach we assume an infinitely large Coulomb interaction and use the QP states which are defined by the canonical transformation which stepwise eliminates the hybridization between the f- and the conduction electrons[39]. The operator form of the effective QP Hamiltonian obtained in such a way is quadratic and the dispersion of the QP states is given by Eq. (38) but the operator algebra is not Fermionic. The charge and heat current density operators are highly non-trivial in the QP representation and it is not clear that they satisfy the Jonson-Mahan theorem nor that the canonical expression in Eq. (13) for the Seebeck coefficient holds. To avoid these difficulties we use the QP representation to estimate the Fermi momentum of the interacting system but calculate the heat and charge currents for the initial model, where the Jonson-Mahan theorem is easily proved. We then use the DMFT self-consistency condition to relate the width and the position of the Kondo resonance to the renormalized c- and f-DOS, which allows us to calculate the transport relaxation time.

2. *Anderson model - 'poor man's approach'*

At elevated temperature, the FL law (42) breaks down and the temperature dependence of $\alpha(T)$ cannot be obtained without numerical methods. However, the periodic Anderson model in the presence of nonzero CF splitting or for large degeneracy cannot be solved exactly by the DMFT mapping and to estimate $\alpha(T)$ we use a 'poor man's mapping'. We assume that the conduction electrons scatter incoherently on the $4f$ ions and calculate the transport relaxation time in the T-matrix approximation. We write $\Sigma_c(k,\omega^+) \simeq n_i T_{kk}(\omega^+)$, where $T_{kk}(\omega^+)$ is the single-ion scattering matrix evaluated on the real axis, and set the concentration of $4f$ ions to $n_i = 1$. Since transport integrals are restricted to the Fermi window, we average $\Sigma_c(k,\omega^+)$ over the FS and write

$$\frac{1}{\tau(\omega)} = -Im\ \Sigma_c(\omega^+). \tag{43}$$

In the case of a single scattering channel (no CF splitting) the vertex corrections vanish by symmetry and the conduction electron's self energy in Eq. (43) is given by $\Sigma_c(\omega^+) = V^2 G_f(\omega^+)$, where $G_f(\omega^+)$ is the retarded Green's function of the effective $\mathcal{L}$-fold degenerate single impurity Anderson model. In the case when the degeneracy is lifted by the CF splitting the vertex corrections do not vanish but we neglect them anyway and use

$$\Sigma_c(\omega^+) = \sum_{\Gamma} V_{\mathbf{k}\Gamma_i} G_{\Gamma_I}(\omega^+) V_{\Gamma_i \mathbf{k}'}. \tag{44}$$

$V_{\Gamma\mathbf{k}} = \langle \Gamma | V | \mathbf{k} \rangle$ is the matrix element for the scattering between the conduction state $\mathbf{k}$ and the f-state belonging to the irrep Γ, and $G_\Gamma(\omega^+)$ is the corresponding Green's function of the single impurity Anderson model with the CF splitting. We calculate $G_\Gamma(\omega^+)$ by the NCA and obtain $\alpha(T)$ from Eqs. (13) and (24). (For details regarding the thermopower obtained by the NCA see Refs. 41 and 22.)

The single impurity Anderson model which approximates the periodic model used in the 'poor man's mapping' is completely different from the auxiliary impurity model in the DMFT approach. The conduction electrons of the former participate in the charge and heat transport and couple to the f-states and the external fields. The density of these states is parameterized by some simple function (square-root or Lorentzian), which is independent of pressure or temperature. Furthermore, the hybridization strength, as parameterized by Γ also is independent of temperature, although it might change with pressure. On the other hand, the conduction states of the auxiliary impurity model used in the DMFT mapping do not couple to external fields and have no direct physical meaning. The auxiliary c-DOS usually does change with both pressure or temperature (i.e. $\Delta_0 \neq \Gamma$ in general).

We expect the 'poor man's mapping' to provide a reliable solution of the periodic Anderson model at temperatures at which the mean free path of conduction electrons is sufficiently short, such that the coherent scattering can be neglected. Recent solution of the spin-1/2 model obtained by the DMFT+NRG shows[18] that the electrical resistance $\rho(T)$ increases rapidly and is very large at the temperature T_K at which $\alpha(T)$ has a maximum. For $T \geq T_K/2$ the DMFT+NRG shows that $\alpha(T)$ is very similar to the exact results[29] obtained for the single impurity spin-1/2 Anderson model. This indicates that the 'poor man's mapping', which neglects the coherent scattering, is reliable above the FL regime and that it can be used to approximate $\alpha(T)$ for $T \geq T_K/2$. However, the single impurity model has to be solved by methods which can deal with large Coulomb correlation and the CF splitting.

The experimental results on the heavy Fermion and valence fluctuators provide additional support for the single impurity approach. The data show that the residual resistance of ternary and quaternary compounds like $EuCu_2(Ge_{1-x}Si_x)_2$, $CePt_{1-x}Ni_x$ and $YbIn_{1-x}Ag_xCu_4$ grows rapidly with x and for $0.3 \leq x \leq 0.8$ the mean free path is reduced by disorder to about a single lattice spacing. In these random alloys the electron propagation is incoherent even at $T = 0$ and they are very well described by the single impurity model. At low doping and in stoichiometric heavy Fermion compounds with small ρ_0 the impurity description breaks down in the low-temperature regime. However, in these systems $\rho(T)$ and $\alpha(T)$ grow

rapidly towards room temperature (RT) and attain large maxima at T_K^ρ and T_K, respectively. In the case of the f-ions with degenerate f-states or a small CF splitting, the data show[5,53,54] $T_K^\rho < T_K < RT$ and we find that above $T_K^\rho/2$ there is not much difference between $\alpha(T)$ of the stoichiometric compounds and doped systems. In the presence of a CF splitting, $\rho(T)$ has two maxima: a low-temperature one at T_K^ρ and a high-temperature one at T_ρ. The thermopower of these systems exhibits two maxima as well[44]: a low-temperature one at $T_K > T_K^\rho$ and a high-temperature one at T_S. The values of $\alpha(T)$ at T_K and T_S are α_K and α_S, respectively. Since the mean free path is short for $T \geq T_K/2$, it is not really surprising that the thermopower of periodic systems and random alloys have the same qualitative features above the FL regime. The experimental data also show that the functional form of $\alpha(T)$ is strongly affected by pressure or chemical pressure. The fact that all the qualitative features of the pressure-induced variations of $\alpha(T)$ are completely accounted for by the 'poor man's mapping' justifies, a posteriori, the approximation which neglects the coherent scattering of conduction electrons on the lattice of f-ions.

In what follows, we discuss the temperature and pressure dependence of $\alpha(T)$ above the FL regime using the NCA solution of the asymmetric single impurity Anderson model with infinite f-f correlation. We assume that pressure or doping increase the coupling constant g and reduce n_f but do not substantially change the CF splitting Δ_{CF}. In the limit of large asymmetry and infinite correlation, the single impurity Anderson model has a universal low-temperature scale, given by the Kondo temperature T_K, which is uniquely related to n_f. Large degeneracy and small CF splitting lead to large T_K which can be further increased by reducing n_f. A small Kondo scale is found for low degeneracy or large CF splitting, which reduces the effective degeneracy of the f-state; the lowest T_K is found for $n_f \simeq 1$.

We consider first the case of a $\mathcal{L}$-fold degenerate f-state and show the typical NCA results[22,41,42] obtained for $\mathcal{L}$=8 in Fig. 2, where $\alpha(T)$ is plotted as a function of temperature for several values of E_f and for constant Γ. The thermopower is characterized by the maximum α_S at temperature $T_S \simeq T_K$. The Kondo scale of the $\mathcal{L}$-fold degenerate Anderson impurity model[40] is $T_K = 3\gamma/\pi k_B$, where $\gamma = (\pi^2 k_B^2/3)\mathcal{L}\rho_f(\mu)Z_f^{-1}$ is the impurity contribution to the specific heat coefficient and $\rho_f(\mu) = (1/\pi\Gamma)\sin^2(\pi n_f/\mathcal{L})$ is the f-DOS of a given symmetry at the Fermi level. Above T_K the thermopower decreases with temperature but the details depend strongly on n_f. For $n_f \simeq 1$, the thermopower has a large high-temperature slope, changes sign at $T_0 > T_K$ and assumes large negative values above T_0. For $0.75 \leq n_f < 1$, the values of T_S and T_0 are increased, while the slope of $\alpha(T)$ above T_S is reduced. In this parameter range n_f is temperature-dependent and to characterize the system we use $n_f(T_K)$. Eventually, for $n_f < 0.7$, we still find a shallow maximum of $\alpha(T)$ below RT but the high-temperature slope is very small and the sign-change does not occur. A similar behavior is obtained if the coupling constant g is reduced by increasing Γ. The thermopower calculated for smaller $\mathcal{L}$ has a lower maximum α_S which occurs at lower temperature T_S[44].

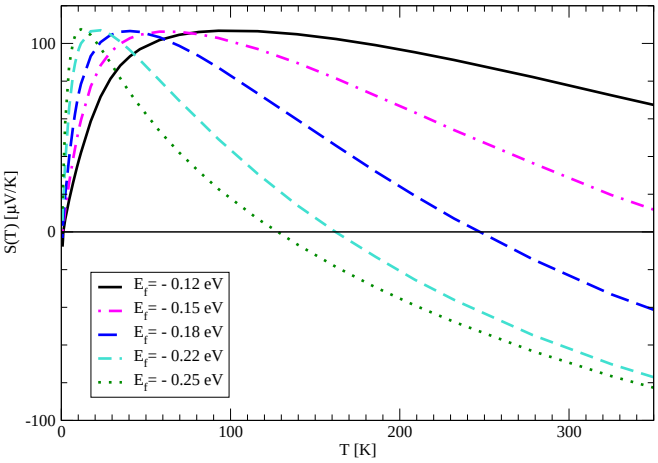


FIG. 1: Thermopower of the single impurity Anderson model of a 8-fold degenerate f-state is calculated by the NCA for fixed hybridization $\Gamma = 0.015$ eV and plotted as a function of temperature for several values of E_f, as indicated in the figure. The values of $n_f(T_K)$ are 0.76, 0,81, 0,.86 0.91, and 0.93 for $-E_f$ =0.12, 0.15, 0.18, 0.22, and 0.25, respectively.

The CF splitting leads to additional features which we explain by the example of an f-ion with two CF states separated by Δ_{CF}. The respective degeneracies of the ground and the excited state are $\mathcal{L}_1 = \mathcal{M}$ and $\mathcal{L}_2 = \mathcal{M}'$, and we have $\mathcal{M}+\mathcal{M}' = \mathcal{L}$. The system now has two characteristic low-energy scales: the Kondo temperature T_K and the scale $T_K^{\mathcal{L}} \gg T_K$ which comes into play[43] when the excited CF states become significantly populated at temperature $T_\Delta \simeq \Delta/2$. For $T \geq T_\Delta$, the thermopower can be approximated by the function $\alpha_{\mathcal{L}}(T)$ which describes an effective $\mathcal{L}$-fold degenerate f-state with Kondo temperature $T_K^{\mathcal{L}}$ and exhibits all the typical features discussed in the previous paragraph. For $n_f \simeq 1$, the function $\alpha_{\mathcal{L}}(T)$ has a maximum $\alpha_S^{\mathcal{L}}$ at $T_K^{\mathcal{L}}$; above $T_K^{\mathcal{L}}$, $\alpha_{\mathcal{L}}(T)$ decreases rapidly and changes sign at $T_0^{\mathcal{L}} > T_K^{\mathcal{L}}$. For $0.8 \leq n_f \leq 0.95$, the maximum $\alpha_S^{\mathcal{L}}$ is enhanced and shifted to higher temperatures, the slope of $\alpha_{\mathcal{L}}(T)$ is reduced and $T_0^{\mathcal{L}}$ is higher. For $n_f \leq 0.8$, $\alpha_S^{\mathcal{L}}$ is further enhanced and the sign-change does not occur. Of course, in a system with a CF splitting, $\alpha_{\mathcal{L}}(T)$ has a physical meaning only for $T \geq T_\Delta$. At low temperatures, $T < T_\Delta$, the excited CF states are unoccupied and the properties are determined by the lowest CF state which is $\mathcal{M}$-fold degenerate (typically, $\mathcal{M} \ll \mathcal{L}$). In the temperature range $T_K/2 < T < T_\Delta$, the behavior of a CF split f level is described by an effective $\mathcal{M}$-fold degenerate Anderson model with Kondo scale T_K. All other parameters being the same, the main difference between this effective model and a simple $\mathcal{M}$-fold degenerate model is that $T_K \gg T_K^{\mathcal{M}}$, where $T_K^{\mathcal{M}} = \lim_{\Delta\to\infty} T_K$. The

enhancement of T_K with respect to $T_K^{\mathcal{M}}$ is due to the virtual transitions from the ground to the excited CF states. The thermopower $\alpha_{\mathcal{M}}(T)$ of the effective low-temperature model exhibits the usual Kondo features. For $n_f \simeq 1$, $\alpha_{\mathcal{M}}(T)$ has a maximum at T_K and changes sign at $T_0^{\mathcal{M}} > T_K$. Note, for a CF doublet and $n_f \simeq 1$, the low-temperature maximum of $\alpha(T)$ could be very small[44]. For $0.7 \leq n_f \leq 0.95$, the maximum of $\alpha(T)$ is enhanced, the slope above the maximum is reduced, and the sign-change is shifted to $T_0^{\mathcal{M}} \gg T_K$. For $n_f \leq 0.7$ the maximum is further enhanced but the sign-change is absent. Of course, for $T \geq T_\Delta$ the excited CF states come into play and $\alpha_{\mathcal{M}}(T)$ ceases to be physically relevant. The overall behavior of $\alpha(T)$ for $T \geq T_K/2$ is now easily obtained by the interpolation.

The NCA calculations break down for $T \ll T_K$ but the initial slope of the thermopower follows from the Sommerfeld expansion, which gives[29]

$$\lim_{T\to 0} \frac{\alpha(T)}{T} = \frac{2\gamma}{|e|n_c} \cot(\frac{\pi n_f}{\mathcal{L}}) \qquad (45)$$

for the $\mathcal{L}$-fold degenerate Anderson impurity model. In the case of CF splitting, the initial slope is obtained by substituting the effective low-temperature degeneracy of the f-state into the above expression, i.e., replacing $\mathcal{L}$ by the degeneracy of the lowest CF state $\mathcal{M}$. Since the on-site correlation is infinitely large and the model is far away from the electron-hole symmetry, the initial slope of $\alpha(T)$ is finite, even for the ground state doublet; it is positive for Ce and Eu ions, which have an additional electron in the magnetic configuration, and is negative for Yb ions, which are magnetic due to an additional hole. However, for $\mathcal{L} = 2$ and $n_f \simeq 1$ the thermopower could be very small. To estimate the magnitude of initial slope we have to take into account that γ decreases exponentially as $\mathcal{L}$ increases or n_f decreases. At constant $\mathcal{L}$, we find that $\alpha(T)/T$ decreases with the reduction of n_f, which is consistent with the NCA results shown in Fig. 1. The dependence of $\alpha(T)/T$ on the effective degeneracy of the f-level and n_f is complicated by the fact that the two factors in Eq. (45) depend strongly on $\mathcal{L}$ and n_f but their functional form is completely different. Equation (45) and the charge neutrality condition $n = n_f + n_c$ show that the reduction of n_f by pressure or chemical pressure reduces the ratio $q = \lim_{T\to 0} \alpha(T)/\gamma T$. Contrary to periodic systems, in random alloys this reduction can be quite large. Note, Eqs. (45) and (42) give opposite slopes for $q(n_f)$.

The above results, obtained for the CF split Anderson model, explain in simple terms the seemingly complicated behavior of $\alpha(T)$ in many heavy Fermions and valence fluctuators with Ce ions. The typical NCA results for the model with a ground state doublet at energy $E_f < 0$ and an excited quartet at energy $E_f + \Delta_{CF}$ is shown in Fig. 2. Various shapes of $\alpha(T)$ are obtained by changing the hybridization $\Gamma(p)$, which mimics the effects of pressure or chemical pressure. The CF splitting Δ_{CF} is the same for all curves but pressure increases the coupling

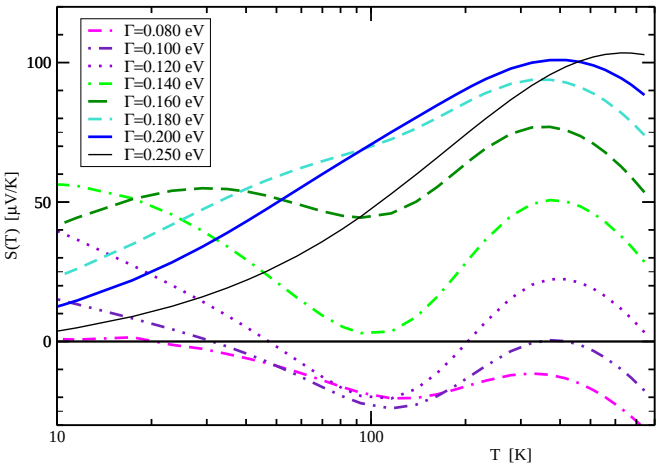


FIG. 2: Thermopower of an f-ion with the ground state doublet and excited quartet calculated by the NCA for the CF splitting $\Delta = 0.07$ eV is plotted as a function of temperature for several values of the hybridization strength Γ, as indicated in the figure. The two bottom curves describe the type (a) Kondo system, the third curve from the bottom is type (b), the two middle curves are type (c) and the third one from the top describes the type (d) Kondo systems. The two upper curves are type (e) and describes valence fluctuators.

constant and the Kondo scale, transfers the f-electrons in the conduction band and reduces, eventually, the effective degeneracy of the f-state. As discussed in detail below, the qualitative features at each pressure (Γ) are easily explained by approximating $\alpha(T)$ by $\alpha_{\mathcal{M}}(T)$ at low temperatures and by $\alpha_{\mathcal{L}}(T)$ at high temperatures. The details of the crossover at $T \simeq T_\Delta$ require numerical calculations but the crossover region is quite narrow and the overall features are easily obtained by interpolation.

Suppose, at ambient pressure g is small enough to give $0.95 \leq n_f \leq 1$. The NCA shows that the spectral function of such a model has well defined CF excitations[22,41] separated by Δ_{CF} and that the low-energy scales satisfy $T_K \ll T_K^{\mathcal{L}} \ll T_\Delta$. For $T \leq T_K$ we expect $\alpha(T)$ with a small maximum α_K at T_K[44]. Above T_K, $\alpha(T)$ decreases and changes sign at $T_0 \simeq 2T_K$. Nothing particular happens at $T \simeq T_K^{\mathcal{L}}$ where the excited CF states are still unoccupied. At T_Δ, the excited CF states become thermally populated and the functional form of $\alpha(T)$ changes from $\alpha_{\mathcal{M}}(T)$ to $\alpha_{\mathcal{L}}(T)$. At ambient pressure and $n_f \simeq 1$ we have $\alpha_{\mathcal{M}}(T) < \alpha_{\mathcal{L}}(T) < 0$ for $T \simeq T_\Delta$, i.e., $\alpha_S \leq 0$ at the high-temperature maximum. The thermopower exhibiting these features is shown by the two lowest curves in Fig. 2 and is classified[21,22] as type (a).

If pressure or chemical pressure increases $\Gamma(p)$ and $g(p)$ such that $0.8 \leq n_f \leq 0.95$, the NCA shows that the low-energy CF excitations are still well resolved and $T_K(p) < T_K^{\mathcal{L}}(p) < T_\Delta$. The maximum of $\alpha(T)$ at T_K is shifted to higher temperatures with respect to the $p = 0$ case, we find $\alpha_{\mathcal{M}}(p, T) > \alpha_{\mathcal{M}}(T)$ for $T \geq T_K(p)$, and have $T_0^{\mathcal{M}}(p) \gg T_K(p)$. The crossover starts at T_Δ but $T_K^{\mathcal{M}}(p)$, $T_0^{\mathcal{M}}(p)$ and $T_K^{\mathcal{L}}(p)$ are now much closer to T_Δ. Since

$\alpha_{\mathcal{M}}(p, T_\Delta)$ and $\alpha_{\mathcal{L}}(p, T_\Delta)$ are enhanced with respect to the $p = 0$ values, pressure brings the two maxima of $\alpha(T)$ closer together, shrinks the temperature interval in which $\alpha(T) < 0$, enhances α_S but does not change T_S. These features are demonstrated by the $\Gamma = 0.12$ curve in Fig. 2, which is classified as type (b).

In the pressure range such that $0.75 \leq n_f \leq 0.8$ the temperature of the sign-change is pushed up and at large enough pressure we get $T_0^{\mathcal{M}}(p) \simeq T_\Delta$. The crossover starts from $\alpha_{\mathcal{M}}(T_\Delta) \geq 0$ and $\alpha(T)$ still exhibits two peaks but is always positive. These features are demonstrated by the $\Gamma = 0.14$ and $\Gamma = 0.16$ curves in Fig. 2, which are classified as type (c). A further increase of pressure leads to $0.7 \leq n_f \leq 0.75$, which shifts $T_K(P)$ close to T_Δ and the two peaks cannot be resolved any more. $\alpha(T)$ exhibits a single peak with a shoulder on the low-temperature side, as shown by the $\Gamma = 0.18$ curve in Fig. 2, which are classified as type (d). Note, as long as the low-energy CF excitations are well defined $\alpha(T)$ has a high-temperature peak at $T_S \simeq T_\Delta$, which is pressure independent, with the maximum value α_S, which is pressure-dependent.

If pressure reduces n_f below 0.7, the NCA calculations show that the CF excitations are absent in the spectral function and $\alpha(T)$ exhibits the same behavior as a fully degenerate *f*-level. In this pressure range, $\alpha(T)$ has a single maximum and the difference with respect to Kondo systems with well-resolved CF excitations is that an increase of pressure shifts T_S to higher temperatures but does not change the magnitude of α_S. These features are typical of valence fluctuators and are demonstrated by the $\Gamma = 0.14$ and $\Gamma = 0.16$ curves in Fig. 2, which are classified as type (e). The curves in Fig. 1 are also of this type. They describe a system without CF splitting such as Eu intermetallics. The Yb systems are characterized by an *f*-hole and a qualitative features of $\alpha(T)$ are obtained by reflecting ('mirror imaging') the curves in Fig. 1 and Fig. 2 about the temperature axis.

The NCA solution provides a reliable description of the experimental data for $T \geq T_K/2$, where the resistivity is large and the mean free path is short. To obtain the overall temperature dependence of the thermopower of the periodic systems we interpolate between the solution obtained by the 'poor man's mapping' and the coherent FL solution described by Eq. (42). In random alloys the low-temperature behavior is described by a local FL and $\alpha(T)$ is obtained by interpolating between Eq. (45) and the NCA result.

3. Falicov-Kimball model

In heavy Fermions described by the periodic Anderson model, the entropy is reduced at the crossover from the high-temperature paramagnetic phase to the low-temperature FL phase. In these systems, the screening of local moments due to the Kondo effect does not affect n_f, which is nearly temperature independent. However, in some Eu and Yb systems, like $EuCu_2Ni_2$ or $YbInCu_4$, the magnetic moment disappears due to a temperature-induced change in n_f, i.e., the entropy is reduced by a valence-change transition. These systems can be described by the Falicov-Kimball model[45] which takes a lattice of localized *f*-sites, which can be either occupied or empty, and conduction states which are delocalized via a nearest-neighbor hopping. The two types of electrons interact via a short-range Coulomb interaction and share a common chemical potential, which controls the total number of electrons $n = n_c + n_f$. The occupation of the *f*-states, which can be split into several CF levels, is restricted to $n_f < 1$. For a given total number of electrons, thermal fluctuations change the average *f*-occupation by transferring electrons or holes from the conduction band to the *f*-states and *vice versa*[33]. The transport coefficients are obtained in the limit of infinite dimensions by substituting the exact conduction electron Green's function into Eq. (15) and integrating Eq. (13) numerically[34,46]. This procedure allows us to discuss not only the dirty FL regime but also the metal-insulator transition.

The $YbInCu_4$-like intermetallics are described by the Falicov-Kimball model, with the interaction large enough to open a gap in the conduction band. We also assume that at low temperatures μ is within the lower (or upper) Hubbard band, so that the ground state is metallic. Since the model neglects quantum fluctuations, the ground state has no *f*-holes and the conduction electrons are essentially free, such that $q \simeq 1$. At finite temperature, the ν-fold degenerate *f*-states become fractionally occupied and the additional paramagnetic entropy of these excited states competes for the free energy with the excitation energy, the kinetic energy of the conduction electrons, and the interaction energy[45]. This gives rise to a valence transition at a temperature T_V, such that a substantial number of electrons (in Eu compounds) or holes (in Yb compounds) are transferred from the conduction band to the $4f$ ions. The onset of the $4f$ paramagnetism is accompanied by the reconstruction of the interacting density of conduction states and the shift of μ into the gap.

We find[34,46] that the electrical resistance of the paramagnetic phase is large and has a maximum at a temperature $T^* \gg T_V$, which is of the order of the gap, or the pseudogap in the density of states. The thermopower obtained by the DMFT is weakly temperature dependent and its sign depends on the band filling. The maximum of $\alpha(T)$ is also at T^*. The overall entropy of the high-temperature phase is very large due to the contribution of local moments and $\tilde{q} \ll 1$. In systems with a valence change transition, $\tilde{q}$ increases sharply to $q \simeq 1$ as temperature is reduced below T_V, indicating the onset of the free Fermi gas phase and the change of the Fermi volume. At intermediate temperatures the behavior can be quite complex[34,46], because both the degeneracy of the *f*-states and the number of charge carriers change at T_V.

By choosing the parameters of the model so as to increase the occupancy of the *f*-states one can stabilize the gapped phase, for large Coulomb repulsion, all

the way down to zero temperature[46]. Calculating the thermopower for the spinless Falicov-Kimball model on a Bethe lattice gives[47] a thermopower that diverges as $\alpha(T) \simeq \Delta/T$, where Δ is the value of the gap. For an intrinsic semiconductor with a density of states increasing as a power law, and assuming that the frequency dependent conductivity is proportional to the density of states, we find[46] $\alpha(T) \simeq \ln T$. In both cases, the corresponding conductivity decays exponentially, so that the entropy current density generated by the applied field, $\mathcal{S}(T) = \alpha(T)\sigma(T)(-\nabla\phi)$, vanishes in the limit $T \to 0$, as required by the third law of thermodynamics[27,48]. This example shows that the value of the q-ratio of a correlated insulator or semiconductor can become very large at low temperatures.

By tuning the parameters of the periodic Anderson model or the Falicov-Kimball model, the system can be brought into the vicinity of a quantum critical point, where strong non-FL features are expected. Such a situation has been considered by Paul and Kotliar[49], who computed the entropy and the thermoelectric power of a system of quasiparticles scattered by two-dimensional spin-fluctuations. They find $\alpha(T) \sim T \ln T$ and $\mathcal{S}_N(T) \sim T \ln T$ but, unfortunately, do not discuss the order of magnitude of $\alpha(T)/\mathcal{S}_N(T)$.

IV. DISCUSSION OF THE EXPERIMENTAL DATA

In this section, we use the theoretical results obtained for the periodic Anderson and the Falicov-Kimball models to discuss the temperature and doping dependence of $\alpha(T)$ and $\alpha/\gamma T$ for several intermetallic compounds with Eu, Ce, and Yb ions. In these compounds, chemical substitution modifies the character of the ground state, changes the characteristic temperature and the low-temperature values of $\alpha(T)/T$ and γ by an order of magnitude, strongly modifies the temperature dependence of $\alpha(T)$, but does not significantly change the ratio $\alpha/\gamma T$. Our theory explains the universal low-temperature features and shows that the observed shapes of $\alpha(T)$ are consistent with the ground state properties at each doping level.

4. Chemical pressure effects in $EuCu_2(Ge_{1-x}Si_x)_2$

In $EuCu_2(Ge_{1-x}Si_x)_2$ intermetallics, Ge doping increases the lattice parameter and acts as a negative pressure which reduces the coupling constant and makes the system more magnetic[4,5]. For $x \simeq 1$, the XPS data indicate a significant mixture of Eu^{2+} and Eu^{3+} ions, which is typical for a valence fluctuator. For $x < 1$ the weight of the Eu^{3+} configuration is reduced with respect to that of the Eu^{2+} configurations and for $x \simeq 0$ the XPS signal is dominated by the magnetic Eu^{2+} ions. At the critical concentration $x_c = 0.65$, there is a change from a FL to an antiferromagnetic (AFM) ground state. Thus, doping changes the magnetic character of the Eu ions.

The doping dependence of the q-ratio for $x > x_c$ can be explained by the periodic Anderson model which takes into account the 8-fold degeneracy of the Eu^{2+} ions but neglects the excited magnetic states of the Eu^{3+} configuration. In $EuCu_2Si_2$, the initial slope of $\alpha(T)$ is small, $\alpha/T = 0.64\ \mu V/K^2$, the specific heat is featureless with a small linear coefficient, $\gamma = 0.065\ J/K^2$ mole, and the q-ratio[5] is $q|_{x=1} = 0.94$. For $0.90 \geq x \geq 0.65$, the γ value increases with Ge-doping and for $x = 0.7$, we find $\alpha/T = 2.86\ \mu V/K^2$, $\gamma = 0.226\ J/K^2$ mole, and $q|_{x=.7} = 1.21$. The slight enhancement of $q(x)$ obtained for $x_c < x < 1$ is most likely due to the transfer of electrons from the conduction band into the f-level induced by a negative chemical pressure. The observed trend agrees with Eq. (42), which predicts that a reduction of the charge carrier density increases the q-ratio. It seems that $q(x)$ increases more rapidly as we approach the AFM transition from the paramagnetic side, but the concentration dependence would have to be fine-tuned, before a more quantitative conclusion could be reached.

The temperature dependence of $\alpha(T)$ at various doping levels is consistent with the magnetic character of the Eu ions. Since $\rho(T)$ increases rapidly with doping and temperature, we use the 'poor man's mapping' and describe the temperature-dependence of the thermopower of $EuCu_2(Ge_{1-x}Si_x)_2$ by the NCA solution of the 8-fold degenerate single impurity Anderson model. The qualitative features of the solution are shown in Fig. 1, where the curves with the highest T_S and lowest n_f corresponds to the Si-rich compound. The Ge-doping reduces n_f, as indicated in the figure. The curves shown in Fig. 1 capture the qualitative features of the experimental data but the quantitative analysis has to take into account the non-resonant scattering channels and use the Nordheim-Gorter rule[42]. This gives $\alpha(T) = \alpha_{NCA}(T)\rho_{NCA}(T)/\rho_{tot} + \alpha_0\rho_0/\rho_{tot}$, where $\rho_{tot} = \rho_0 + \rho_{NCA}$ and α_0 is the thermopower due to the non-magnetic scattering. In $EuCu_2(Ge_{1-x}Si_x)_2$, the potential scattering is large but α_0 is small, and the main effect of the Nordheim-Gorter rule is an effective reduction of the magnetic contribution.

At the Si-rich end, $0.9 \leq x \leq 1$, the experimental data show that $\alpha(T)$ is always positive. After an initial linear increase $\alpha(T)$ reaches a broad maximum, $\alpha_S > 40\ \mu V/K$, at a temperature $T_S \geq 125$ K. The value of α_S does not change much, while T_S is reduced and the low-temperature slope of $\alpha(T)$ is enhanced with Ge-doping. These changes can be understood in terms of pressure effects discussed in Sec. III.2 (see Fig. 1). For $x \simeq 1$ the maximum of $\alpha(T)$ occurs at the highest temperatures, the decay of $\alpha(T)$ for $T > T_S(x)$ is rather slow, and no sign-change is observed, which is consistent with the mixed-valent character of the Eu ions and $n_f < 1$. The negative pressure due to Ge-doping increases n_f and stabilizes the magnetic Eu^{2+} configuration. This shifts the maximum of $\alpha(T)$ to a lower temperature, makes the

slope of $\alpha(T)$ above $T_S(x)$ more negative, and gives rise to the sign-change at $T_0(x)$. The data show that Ge doping reduces $T_0(x)$ faster than $T_S(x)$. Such behavior also agrees well with the NCA solution of the Anderson model and allows us to identify $T_S(x) = T_K(x)$ and explain the decrease of $T_0(x)$ by the reduction of the coupling constant.

For $x < x_c$, long-range magnetic order occurs at a Neel temperature $T_N(x)$, as indicated by the anomaly in $C_P(T)$ and a discontinuity in the slope of $\rho(T)$[4,5]. The Neel temperature increases rapidly as x decreases from x_c to $x = 0.5$. In this concentration range, the XPS data indicate[4,5] a strong mixture of Eu^{2+} and Eu^{3+} ions at temperatures below $T_N(x)$, although the Eu^{3+} component is less pronounced than for $x \geq x_c$. The maximum of $T_N(x)$ is reached for $x \simeq 0.5$ and below this concentration, $T_N(x)$ decreases slowly as x is reduced[4]. Note, below 30% of Si the XPS data do not indicate the presence of any Eu^{3+} configuration, which indicates a different magnetic ground state around $x \simeq 0$ than around $x \simeq x_c$.

The magnetic transition is difficult to see in $\alpha(T)$ for $0.6 < x \leq x_c$, where Ge-doping increases T_N, reduces T_K, and sharpens the Kondo maximum of $\alpha(T)$. However, the maximum of $\alpha(T)$ is still fully developed, T_K is close to T_N, and the only effect of the AFM transition on $\alpha(T)$ is a slight change of slope at T_N. For $0.5 \leq x \leq 0.6$, negative pressure reduces $T_K(x)$ below $T_N(x)$, such that $\alpha(T_N) < \alpha_S$ and $\alpha(T)$ acquires a cusp, as its slope changes at T_N from negative (for $T > T_N$) to positive (for $T < T_N$). In this concentration range, $T_N(x)$ is still rather close to $T_K(x)$ and the values of $\alpha(T)$ around $T_N(x)$ are large but the cusp makes the overall shape of $\alpha(T)$ quite different from what one finds in the samples with a FL ground state, where $\alpha(T)$ has a rounded maximum (see Figs. 4 and 7 in Ref. 5). Above $T_N(x)$, the shape of $\alpha(T)$ looks much the same as in the non-magnetic samples well above T_S (see Fig. 6 of Ref. 5). Using the single impurity Anderson model to explain the transport properties of the paramagnetic phase of $EuCu_2(Ge_{1-x}Si_x)_2$ allows us to infer $T_K(x)$ from the shape of $\alpha(T)$ and the value of $T_0(x)$, and compare the concentration dependence of $T_K(x)$ with $T_N(x)$ even for antiferromagnetic samples in which $T_K(x) \ll T_N(x)$. For $x \leq 0.5$, the Ge doping reduces $T_K(x)$ much faster than $T_N(x)$, and the AFM transition occurs at a temperatures comparable to $T_0(x)$. The thermopower anomaly at T_N is now very weak, because for $T \gg T_K$ the Kondo screening is small and $\alpha(T)$ is far away from the Kondo maximum.

To account for the overall temperature and concentration dependence of $\alpha(T)$ in samples with an AFM ground state and $0.5 \leq x \leq x_c$, we note that the Kondo scale is quite large in this concentration range so that the $4f$ moments order magnetically before the entropy is quenched by the Kondo effect. The XPS data indicate a substantial hybridization of the $4f$ and conduction states even below T_N and the hybridized f-electrons contribute to the Fermi volume. We assume that the paramagnetic entropy is removed at T_N by an anomalous spin density wave (SDW) which gaps a part of the FS. Indirect evidence for the SDW transition is provided by the large specific heat and small effective moment in the ordered phase. Direct evidence by neutron scattering data on $EuCu_2(Ge_{1-x}Si_x)_2$ is lacking, but the SDW transition has been seen recently in high-pressure neutron data[50] on the 'reduced-moment' antiferromagnet $CePd_2Si_2$. (Unfortunately, the high-pressure thermopower and the specific heat data on this compound are not available.) Note, the maximum of $\gamma(x)$ and the initial slope of $\alpha(T)$ is at $x_c = 0.65$, while $T_N(x)$ has a maximum at $x = 0.5$. The non-monotonic behavior of $T_N(x)$ and of the AFM transition below T_K are difficult to explain in terms of the simple Doniach diagram, which considers the scattering of conduction electrons on a lattice of localized spins and predicts that $\gamma(x)$ and $T_N(x)$ should peak at x_c.

If we assume that the thermopower tracks the entropy of the charge carriers, the large value of $\alpha(T)$ found for $0.55 \leq x \leq 0.65$ points to a large hybridization below T_N. The small values of $\alpha(T)$ found for $x \leq 0.5$ indicate that the coupling between the f and conduction states is reduced by negative chemical pressure. At the Ge-rich end, the hybridization and the Kondo coupling seem to be small and the f-electrons are completely localized. For $x \leq 0.3$ the magnetic state involves the unscreened local moments of the Eu^{2+} ions. Below T_N, the conduction states are effectively free, except for scattering off of spin waves. The low-temperature entropy is dominated by the linear conduction-electron contribution and $\alpha(T)$ is too small to show an anomaly at T_N.

5. *Chemical pressure effects in $CePt_{1-x}Ni_x$ intermetallics*

For our next example, we consider the doping effects on $\alpha(T)$ and $\alpha/\gamma T$ in $CePt_{1-x}Ni_x$. For $x \geq 0.95$, this system is a valence fluctuator with a FL ground state and for $x < 0.95$ a heavy Fermion with a ferromagnetic (FM) ground state[6,7,51]. The temperature and concentration dependence of $\alpha(T)$ in the paramagnetic phase show all the typical features of a Ce ion with a CF split f-state, as discussed in detail in Sec. III.2. The CF splitting is estimated to be about 200 K and T_Δ is about 100 K[51]. We account for the observed behavior assuming that the expansion of the volume due to Pt doping[51] reduces hybridization and the coupling constant but does not change Δ_{CF}. The qualitative features of the thermopower agree with the schematic results shown in Fig. 2 but for a quantitative agreement we should use the appropriate CF scheme and tune the model parameters.

For $0.9 \leq x < 1$, we find the FL features at low temperatures, a maximum α_S at $T_S \simeq 120$ K, and a slow decay of $\alpha(T)$ above T_S. Pt doping shifts T_S from 120 K to 100 K without significant change to α_S, as described by the type (e) curves in Fig. 2. Such behavior is typical of valence fluctuators with a single low-energy scale and n_f too small for the CF excitations to appear[52].

We estimate the initial slope of $\alpha(T)$ for $x = 0.95$ to about[6] $\alpha/T \simeq 3$ μV/K^2 and the specific heat coefficient to $\gamma = 0.120$ J/K^2 mole[7], which gives $q|_{0.95} \simeq 2.4$.

For $0.75 \leq x \leq 0.95$ a new feature appears and the thermopower assumes first the shape (d) and then type (c). In this concentration range, Pt doping reduces α_S but does not change T_S, which indicates the presence of CF excitations and two (or more) low-energy scales. The high-temperature one, $T_K^{\mathcal{L}}$, characterizes a fully degenerate CF state, and the low-temperature one, T_K, characterizes the CF ground state. To explain the data, we assume $T_K < T_K^{\mathcal{L}} < T_0 \simeq T_\Delta$, which requires $n_f < 1$ (see the discussion in Sec. III.2). At RT all the CF states are equally populated, the *f*-state is effectively $\mathcal{L}$-fold degenerate, and $\alpha(T)$ can be approximated by $\alpha_{\mathcal{L}}(T)$, which is a monotonic function with a negative slope. As the temperature decreases, the excited CF states depopulate and at T_Δ there is a crossover from the high-temperature regime, to the low-temperature one, where the degeneracy of the *f*-state defines the lowest CF state and $\alpha(T) \simeq \alpha_{\mathcal{M}}(T)$. Since $n_f < 1$, $T_0^{\mathcal{M}}$ is comparable to T_Δ and the functional form of $\alpha(T)$ does not change much at the crossover. Negative chemical pressure reduces $T_K^{\mathcal{L}}$ and the (negative) slope of $\alpha_{\mathcal{L}}(T)$ for $T > T_K^{\mathcal{L}}$, such that Pt doping reduces $\alpha_S(x)$. (Note, $T_S \simeq T_\Delta \gg T_K^{\mathcal{L}}$.) However, Δ_{CF} is not changed by doping and the position of the high-temperature thermopower maximum α_S is always at T_Δ. The peculiar feature of $CePt_{1-x}Ni_x$ in this concentration range is the FM transition which occurs at $T_c \simeq T_K$ and is indicated by the discontinuous change in the slope[6,51] of $\alpha(T)$ and $\rho(T)$. (This feature is quite similar to what one finds at the AFM transition in $EuCu_2(Ge_{1-x}Si_x)_2$.) At $x = 0.85$ the thermopower and the specific heat data give $\alpha/T \simeq 4$ μV/K^2[26] and $\gamma = 0.180$ J/K^2 mole[7], such that $q|_{0.85} \simeq 2.1$. Using Eq. (42), one is tempted to associate the reduction of $q(x)$ by Pt doping with the transfer of *f*-electrons into the conduction band. However, the onset of the FM transition makes the estimate of the initial thermopower and the specific heat slope susceptible to large errors and a quantitative analysis is difficult. The low-temperature entropy is now due to the magnetic degrees of freedom and is unrelated to the entropy of the charge carriers.

A further increase in the Pt concentration continuously reduces T_K and increases n_f, which rapidly shifts T_0 to lower temperature, such that $T_0 < T_\Delta$ for $x \simeq 0.5$. Once the high- and low-temperature regimes are sufficiently far apart, a double-peak structure appears in $\alpha(T)$. The high-temperature peak remains at $T_S(x) \simeq T_\Delta$ but $\alpha_S(x)$ is systematically reduced by Pt doping. Considered as a function of temperature, $\alpha(T)$ goes through a minimum for $T < T_S$, and then increases towards S_K, as predicted by the NCA calculations. The minimum of $\alpha(T)$ for $x = 0.5$ does not reach negative values, as shown by the type (c) curve in Fig. 2. For $x < 0.5$ there is a range of temperatures for which $\alpha(T) < 0$, i.e., the type (b) behavior is obtained. The data show that $T_0(x)$ decreases rapidly with Pt doping but the corresponding shift of the low-temperature peak at $T_K(x)$ cannot be observed because the full development of this Kondo peak is intercepted by the FM transition and a cusp in $\alpha(T)$ appears at the transition temperature. (This cusp is similar to what is observed in $EuCu_2(Ge_{1-x}Si_x)_2$ for $x \leq 0.5$.) In summary, the temperature and doping dependence of the Seebeck coefficient of $CePt_{1-x}Ni_x$ in the paramagnetic phase are in complete agreement with the NCA calculations.

The onset of the magnetic transition below T_K and the non-monotonic concentration dependence of $T_c(x)$ are also difficult to understand in terms of the Doniach diagram, obtained by a simple comparison of the Kondo and the RKKY scales. The large values of $\alpha(T)$ at the transition and the similarity to the $EuCu_2(Ge_{1-x}Si_x)_2$ data, can be taken as an evidence that the ferromagnetic transition in $CePt_{1-x}Ni_x$ is also due to an anomalous SDW transition which partly gaps the hybridized FS.

Similar behavior for $\alpha(T)$ is also seen in many other Ce intermetallics like $Ce(Pb_{1-x}Sn_x)_3$ or $Ce(Cu_{1-x}Ni_x)_2Al_3$[3], in which the $\alpha/\gamma T$-ratio is about twice as large as in $EuCu_2(Ge_{1-x}Si_x)_2$. It would be interesting to study $q(x)$ as one approaches the critical concentration from the paramagnetic side and determine whether $q(x)$ exhibits different features above the AFM and the FM transitions.

6. *Chemical pressure effects in $YbIn_{1-x}Ag_xCu_4$ intermetallics*

Another example of chemical pressure effects is provided by $YbIn_{1-x}Ag_xCu_4$ intermetallics[8,9,19] which show anomalous behavior due to the fluctuations of Yb ions between the magnetic Yb^{3+} configuration with a single *f*-hole and non-magnetic Yb^{2+} configurations. Indium doping expands the lattice and increases the weight of Yb^{2+} with respect to Yb^{3+} configuration[20] by transferring the electrons from the conduction band to the 4*f*-state. This reduces the number of *f*-holes and increases the Kondo coupling which makes the compound less magnetic. However, the total number of conduction electrons is increased and the depletion of the conduction band due to chemical pressure is compensated by the substitution of the monovalent Ag by the trivalent In.

We consider, first, the behavior of these compounds in the coherent FL regime. $YbAgCu_4$ is a typical heavy-Fermion with small characteristic temperature[9,19], as indicated by an enhanced Pauli-like magnetic susceptibility, large specific heat coefficient and a large concentration of Yb^{3+} ions. The XPS data show[59] that the number of *f*-holes in the ground state is large $n_f^h > 0.9$. The thermopower and specific heat data give $\alpha/T = 2.2$ μV/K^2 and $\gamma = 0.215$ J/K^2 mole at $T \leq 10$ K, such that $q|_{x=1} = 0.98$. At the In-rich end ($x = 0.4$) the system is a typical valence fluctuator with large characteristic temperature, as indicated by the slowly varying metallic resistivity, weakly enhanced Pauli-like susceptibility and

small specific heat coefficient[58]. The XPS data[19] indicate $n_f^h < 0.9$, i.e., an increased weight of the $4f^{14}$ configuration. The thermopower and specific heat data at 10 K give $\alpha/T = 0.36$ μV/K^2 and $\gamma = 0.036$ J/K^2 mole, such that $q|_{x=.4} = 0.96$. For $0 \leq x \leq 0.4$, the values of α and γ in the FL regime do not show any further changes with doping. Describing the Ag-rich compounds by the periodic Anderson model we find that the doping dependence of q is consistent with Eq. (42) if we take into account that the Ag–In substitution increases the number of conduction electrons despite the charge transfer induced by the negative chemical pressure. Thus, In doping transforms the system from a heavy Fermion into a valence fluctuator and changes the low-temperature value of γ and α/T by an order of magnitude but has only a small effect on the low-temperature ratio $\alpha/\gamma T$. The enhanced thermopower and large specific heat coefficient indicate a large Fermi volume due to the hybridized *f*-states.

The temperature dependence of $\alpha(T)$ is consistent with the ground state properties for each value of x. To start with, notice that the electrical resistance of all these compounds increases rapidly with temperature or doping and that above the FL regime the mean free path is short enough to justify the 'poor man's mapping'. (For $0.3 \leq x \leq 0.8$, the residual resistivity is large and the single impurity approach can be extended down to $T = 0$, i.e., the translationally invariant FL of the periodic system can be replaced by the local FL.) The properties of the stoichiometric compound $YbAgCu_4$ above the FL regime are well described by the NCA solution of a CF split Anderson model with a ground state doublet, and excited quartet and doublet states at 4 meV and 7 meV, respectively[59]. Taking the coupling $g = V^2\mathcal{N}_0(\mu)/|E_f - \mu|$, such that $T_K = 70$ K, we find the ground state value $n_f^h \simeq 0.9$ and the temperature variation $n_f^h(T)$ which agrees with the XPS data[59]. For the same parameters the NCA calculations give $\alpha(T)$ with a deep negative minimum of about $\alpha_S \simeq -30$ μV/K and $T_S \simeq 60$ K. The CF splitting is too small (or g is too large) to produce any discernible CF structure and the overall shape of $\alpha(T)$ is characterized by a single deep minimum. (Note the 'mirror image' analogy with the intermetallic compounds with Ce ions: $\alpha(T)$ is described by the 'mirror image' of the type (d) curve in Fig. 2.) The NCA results agrees with the experimental data on $YbAgCu_4$ which show[9] $\alpha(T)$ with a broad minimum at about $T_S \simeq 50$ K and $\alpha_S \simeq -40$ μV/K. Above T_S the thermopower has a a large positive slope, which is consistent with $n_f^h \simeq 0.9$, and reaches small negative values at RT. For $T \gg T_K$ the *f*-electrons are localized and contribute a large paramagnetic term to the overall entropy (the entropy of the unhybridized conduction electrons is small), so that $\tilde{q} \ll 1$.

For $0.5 \leq x \leq 1$, the experimental data show[9] that In doping shifts $\alpha(T)$ to higher temperatures, such that $T_S(x) > T_S(0)$. The RT values are reduced by doping ($\alpha(T)$ is more negative) but the bare data show $\alpha_S(x) > \alpha_S(0)$. Note, the NCA calculations refer to the magnetic ion contribution and a quantitative comparison would require the Nordheim-Gorter analysis which cannot be performed since the absolute values of $\rho_0(x)$ are not available. The qualitative features of $\alpha(T)$ can be explained by the Anderson model with the same CF level scheme as above but with an enhanced coupling. We describe the negative chemical pressure due to In substitution by shifting the bare *f*-level closer to the chemical potential and keeping the hybridization V unchanged. (For details of the NCA description of Yb compounds see Ref. 22.) Thus, the substitution of Ag by In enhances $g(x)$ and for large enough doping we get $g(x) \simeq 1$, which transforms $YbIn_{1-x}Ag_xCu_4$ into a valence fluctuator. The NCA solution shows that an increase of $g(x)$ enhances $T_K(x)$ and $T_S(x)$ with respect to the $x = 0$ values and reduces the slope of $\alpha(T)$ above $T_S(x)$. This makes the RT values of $\alpha(T)$ more negative, in agreement with the experiment[9]. Using the 'mirror image' analogy with Ce compounds, we see from Fig. 2 that In-doping transforms the type (d) thermopower of a heavy Fermion with large T_K into the type (e) thermopower of a valence fluctuator.

For $x \leq 0.5$, the substitution of monovalent Ag by trivalent In, brings μ and E_f in the vicinity of the band edge E_c which gives rise to completely new features. In this concentration range $YbIn_{1-x}Ag_xCu_4$ is a valence fluctuator and $n_f^h(T)$ is strongly temperature dependent, such that the temperature-induced transfer of *f*-holes in the conduction band can reduce $\mu - E_c$ and $E_f - E_c$ to zero. Once μ is within the gap of the density of states, the effective hybridization is switched off and the magnetic moment of the *f*-ions cannot be quenched by Kondo screening[60,61]. Thus, the transition from the low-temperature coherent FL state to the high-temperature disordered paramagnetic state cannot follow the usual 'Kondo route', taken by the heavy Fermions. The valence fluctuators like $YbIn_{1-x}Ag_xCu_4$ for $x \leq 0.5$, belong to a new class of materials in which the transition between the low- and high-entropy phase is driven by the Falicov-Kimball interaction. This gives rise, at the temperature T_V, to a change in the relative occupancy of the f and the conduction states and an abrupt modification of the properties of the system. The valence change transition is clearly seen in the XPS data; above T_V, the spectra indicate a stable $4f^{13}$ configuration of Yb ions and below T_V one has a mixture of $4f^{13}$ and $4f^{14}$ states[19]. The magnetic character of the Yb ions changes at T_V, as indicated by an abrupt change of the susceptibility from Pauli-like to Curie-like[19]. In the high-temperature phase, the Curie constant is close to the free ion value of Yb^{3+}. The conduction states are also modified at T_V, as indicated by a drastic change of the frequency dependence of the optical conductivity[62] and by a large increase in the resistivity[63]. The electrical resistance and the Hall coefficient of the high-temperature phase of $YbIn_{1-x}Ag_xCu_4$ are typical of narrow-band semiconductors or semimetals with a very low carrier density, and neither the transport nor the thermodynamic properties show any sign

of the Kondo effect. The proximity of μ to E_c is indicated in $YbInCu_4$ by the Hall data and band-structure calculations[63].

The anomalous magnetic response of *f*-electrons and the metal-insulator transition of the conduction states, which is seen in $YbInCu_4$-like systems, are well described by the spin-degenerate Falicov-Kimball model[45]. Performing DMFT calculations for a parameter set which yields the valence change transition at $T_V = 50$ K and opens a pseudogap of the order of $T^* \simeq 500$ K, we obtain the main features of the magnetic susceptibility, the XPS data, and the optical conductivity of $YbIn_{1-x}Ag_xCu_4$ at temperatures above T_V. The calculated thermopower[34] is of the order of a few $\mu V/K$, and its sign is either positive or negative, depending on the band filling and the shape of the conduction band. The proximity of μ to the pseudogap would lead (in a non-interacting system) to a shallow minimum of $\alpha(T)$ at a temperature of the order of T^*, but in an interacting system, the valence-change transition destabilizes the semiconducting phase, and gives rise to a discontinuity of $\alpha(T)$ at T_V. The low-temperature FL state has a large characteristic temperature and $|\alpha(T)|$ is a linearly increasing function of temperature. Thus, a cusp or even a discontinuity appears in $\alpha(T)$ at T_V. Below T_V the entropy of the system is given by the entropy of the conduction states and $q = 1$. Above T_V the entropy is dominated by the contribution of the localized, paramagnetic states, $\mathcal{S} \simeq R \ln 8$, and $\tilde{q} \ll 1$. The large reduction of the $\alpha/\mathcal{S}$ ratio at T_V is an indication of the reduction of Fermi volume.

V. SUMMARY AND CONCLUSIONS

In this contribution, we have discussed recent experiments which report an universal ratio of the low-temperature thermopower and specific heat of heavy Fermion and valence fluctuating intermetallic compounds with Ce, Eu, and Yb ions[1,2,3,4,5,6,7,8,9,10,11,51]. The data analysis has shown[1,2] that systems with very different values of α/T and γ often have similar values of the low-temperature ratio $q = N_A e\alpha(T)/\gamma T$. Here, we considered in some detail the chemical pressure data on $EuCu_2(Ge_{1-x}Si_x)_2$, $CePt_{1-x}Ni_x$, and $YbIn_{1-x}Ag_xCu_4$ intermetallics, in which the character of the ground state is concentration dependent and α/T and γ change by an order of magnitude, while $q(x)$ shows only small, but systematic, deviations from universality.

We have first addressed this problem on a macroscopic level and derived the $\alpha/\gamma T$ ratio from transport equations. Using general thermodynamic arguments, and assuming that charge and heat are transported at low temperatures by quasiparticle currents, we found $q = N_A/N$, where N/N_A is the effective concentration of the charge carriers. However, this derivation also showed that for a general many-body system, the $q = N_A/N$ law is only approximately valid. We have discussed various possible sources for the non-universal behavior and pointed out the difficulties which have to be taken into account when comparing the experimental and theoretical results for systems which are close to a phase boundary.

We have then analyzed the low-temperature behavior of the periodic Anderson and the Falicov-Kimball models using the DMFT approach and found the universal ratio $\alpha/\gamma T$. We have discussed two possible routes which the system can follow to remove the entropy of the paramagnetic states at low temperatures and showed that the ratio of the thermopower and the entropy, $\alpha/\mathcal{S}$, tracks the Fermi volume of the charge carrying states. These results explain the near-universality of the q-ratio observed in $EuCu_2(Ge_{1-x}Si_x)_2$, $YbIn_{1-x}Ag_xCu_4$, and similar systems with a coherent FL ground state. A weak concentration dependence of $\alpha/\gamma T$ is most likely due to the transfer of the charge from the *f*-level to the conduction band or vice versa, as described by the expression in Eq. (42). The $CePt_{1-x}Ni_x$ data also show a slight doping dependence but the onset of the ferromagnetic transition precludes a quantitative analysis. The calculations for correlated insulators, described by the Falicov-Kimball model, show that $q(T)$ can assume very large values at low temperature.

We have also shown, using the 'poor man's mapping' which approximates the periodic lattice of $4f$ ions by the single impurity Anderson model, that the temperature dependence of $\alpha(T)$ in $EuCu_2(Ge_{1-x}Si_x)_2$, $CePt_{1-x}Ni_x$ and $YbIn_{1-x}Ag_xCu_4$[1,3,4,6,8,9] is consistent with the character of the ground state at each doping level. The behavior of $\alpha(T)$ calculated by the NCA for $T \geq T_K/2$ captures the main features of pressure and doping experiments on heavy Fermions and valence fluctuators. Since $\alpha(T)$ does not show much structure for $T \leq T_K/2$, the overall temperature dependence of $\alpha(T)$ is easily obtained, interpolating between the FL and the NCA results. Our calculations explain the drastic doping-induced variation of $\alpha(T)$ observed in many intermetallic compounds with Ce, Yb and Eu ions. They also explain the pressure-induced crossover from a Kondo system with small Kondo temperature due to CF splitting to a Kondo system with large Kondo temperature, and eventually to a valence fluctuator, as observed in the resistivity[12] and thermopower data[13] on $CeCu_2Ru_2$. The double-peak structure of $\alpha(T)$ observed in heavy Fermions (or the single-peak in valence fluctuators) is reproduced well by the NCA results for the single-ion Anderson model with (or without) CF splitting, as shown schematically in Figs. 1 and 2.

In the case of random alloys described by the single impurity Anderson model, the zero-temperature limit of $\alpha/\gamma T$ is given by the expression in Eq. (45) which differs by $\cot(\pi n_f/\mathcal{M})$ from the corresponding expression in Eq. (42) for the Anderson lattice. The impurity result applies to random alloys obtained by the substitutional doping of the rare earth sites, like $Ce_{1-x}La_xB_6$[53,54], $Ce_{1-x}Y_xCu_2Si_2$[55], $Ce_{1-x}La_xCu_2Si_2$[56], $Yb_{1-x}Y_xInCu_4$[57] and similar systems. It might also apply to ternary and quaternary

systems with one rare earth ion per unit cell but a short mean free path. If the effective degeneracy of the *f*-state is changed in random alloys by chemical pressure or pressure, the factor $\cot(\pi n_f/\mathcal{M})$ should lead to observable modifications of the q-ratio. However, the experimental verification is complicated by the fact that the magnetic and non-magnetic contributions to $\alpha(T)$ and $C_V(T)$ are often difficult to separate.

In summary, our results show that the thermopower is a sensitive probe of the low-energy excitations and that the seemingly complicated behavior of $\alpha(T)$ can be explained in simple terms. It is interesting to note that the expressions in Eqs. (45) and (42), combined with the charge neutrality condition $n = n_f + n_c$, give a zero-temperature q-ratio which is different for periodic systems and random alloys. The experimental situation could be clarified by measuring α/T and C_P/T at various hydrostatic pressures on a single stoichiometric sample with low residual resistance. Pressure can change the effective degeneracy of the ground state, increase or reduce the characteristic temperature of a given compound by several orders of magnitude and provide a crucial test for the 'universality' of the $\alpha/\gamma T$-ratio. Pressure also has a dramatic effect on the overall shape of $\alpha(T)$ and we hope that the thermopower and specific heat data of of heavy Fermion single crystals taken under hydrostatic pressure will soon be available. Finally, it would be interesting to follow the behavior of the q-ratio as a paramagnetic system approaches a magnetic transition or a metal-insulator transition gives rise to large changes in the Fermi volume.

Acknowledgments

This work has been supported by the Ministry of Science of Croatia (MZOS, grant No. 0035-0352843-2849), the COST P-16 ECOM project, the DFG grant No: Dr274/10-1, and the National Science Foundation (grant No. DMR-0210717). Useful discussions with Z. Hossain, C. Geibel, J. Sakurai, K. Behnia, J. Flouquet, I. Aviani, M. Očko and B. Horvatić are gratefully acknowledged.

[1] J. Sakurai, in *Transport and Thermal Properties of f-electron Systems*, ed. G. Oomi et al. (Plenum Press, NY, 1993), p.165.
[2] K. Behnia, D. Jaccard and J. Flouquet, J. Phys, C: Condensed Matt. **16**, 5187, (2004).
[3] J. Sakurai and Y. Isikawa, J. Phys. Soc. Japan **74**, 1926 (2005).
[4] S. Fukuda, Y. Nakanuma, J. Sakurai, A. Mitsuda, Y. Isikawa, F. Ishikawa, T. Goto and T. Yamamoto, J. Phys. Soc. Japan **72**, 3189 (2003).
[5] Z. Hossain, C. Geibel, N. Senthilkumaran, M. Deppe, M. Baenitz, F. Schiller, and S. L. Molodtsov, Phys. Rev. B **69**, 014422 (2004).
[6] J. Sakurai, A. Iwasaki, Q. Lu, D. Ho, Y. Isikawa, J. R. Fernández, and C. Gómez Sal, J. Phys. Soc. Japan **71**, 2829 (2002).
[7] J. E. Espeso, J. C. Gomez Sal, and J. Chaboy, Phys. Rev. B **63**, 014416 (2000).
[8] M. Očko, Dj. Drobac, J. L. Sarrao, Z. Fisk, Phys. Rev. B **64**, 085103 (2001).
[9] M. Očko, J.L. Sarrao, Ž. Šimek J. Mag. Mag. Mater. **43-46**, 284 (2004).
[10] J. Benz, C. Pfleiderer, O. Stockert and H. v. Löhneysen, Physica B **259-261**, 380 (1999).
[11] H. v. Löhneysen, T. Pietrus, G. Portisch, H. G. Schlager, A. Schröder, M. Sieck, and T. Trappmann, Phys. Rev. Lett. **72**, 3262 (1994).
[12] H. Wilhelm and D. Jaccard, Phys. Rev. B **66**, 064428 (2002).
[13] H. Wilhelm, D. Jaccard, V. Zlatić, R. Monnier, B. Delleyand, and B. Coqblin, J. Phys.: Condens. Matter **17**, S823 (2005).
[14] N. W. Ashcroft and N. D. Mermin, *Solid State Physics*, Chapter 13 (Saunders, Philadelphia, 1976).
[15] A. F. Ioffe, *Semiconductors, Thermoelements and Thermoelectric Cooling* (Infosearch, Ltd., London, 1957).
[16] K. Miyake and H. Kohno, J. Phys. Soc. Japan **74**, 254 (2005).
[17] G. D. Mahan, *Many-Particle Physics* (Plenum, New York, 1981).
[18] C. Genzebach, F. B. Anders, G. Czycholl, and T. Pruschke, Phys. Rev. B **74**, 195119 (2006)
[19] A.L. Cornelius, J.L. Lawrence, J.L. Sarrao, Z. Fisk, M.F. Hundley, G.H. Kwei, J.T. Thompson, C.H. Booth, F. Bridges, Phys. Rev. B **56**, 7993 (1997).
[20] J. L. Sarrao, C. D. Immer, C. L. Benton, Z. Fisk, J. M. Lawrence, D. Mandrus and J. D. Thompson, Phys. Rev. B **54**, 12207 (1996).
[21] P. Link, D. Jaccard, and P. Lejay, Physica B **225**, 207 (1996).
[22] V. Zlatić and R. Monnier, Phys. Rev. B **71**, 165109 (2005).
[23] H. B. Callen, Phys. Rev. **73**, 1349 (1949).
[24] J. M. Luttinger Phys. Rev. **135**, A1505 (1964).
[25] Following Luttinger[24], we use the Coulomb gauge and couple the external potential to the charge density. The coefficient of the thermal gradient is not calculated directly from the quantum mechanical averages (thermal force does not appear in the Hamiltonian) but follows in an indirect way[24]. The perturbation expansion is performed for the Hamiltonian which includes a small gravitational field and the coefficient of the thermal gradient is identified with the correlation function multiplying the gradient of the gravitational potential.
[26] C. A. Domenicali Rev. Mod.Phys. **16**, 237 (1954).
[27] E. M. Lifshitz, L. D. Landau, and L. P. Pitaevskii, *Electrodynamics of Continuous Media* (Elsevier Butterworth-Heinemann, Oxford, 1984).
[28] L. Onsager, Phys. Rev. **37**, 405 (1931).
[29] T. Costi, A. Hewson, and V. Zlatić, J. Phys, C: Condens. Matter **6**, 2519 (1994).

[30] R. D. Barnard, *Thermoelectricity in Metals and Alloys* (Taylor and Francis, London, 1972)

[31] C. L. Kane and M. P. A. Fisher, Phys. Rev. Lett. **76**, 3192 (1996).

[32] G. D. Mahan, in *Solid State Physics*, (Academic Press, San Diego, 1998), Vol. **51**, p. 81.

[33] J. K. Freericks and V. Zlatić, Rev. Mod. Phys. **75**, 1333 (2003).

[34] J. K. Freericks and V. Zlatić, Phys. Rev. B **64**, 245118 (2001).

[35] W. Metzner and D. Vollhardt, Phys. Rev. Lett. **62**, 324 (1989).

[36] U. Brandt and C. Mielsch, Z. Phys. B **75**, 365 (1989)

[37] A. Georges, G. Kotliar, W. Krauth, and M. J. Rozenberg, Rev. Mod. Phys. **68**, 13 (1996).

[38] A. Khurana, Phys. Rev. Lett. **64** 1990 (1990)

[39] A. Hübsch and K.W. Becker, Eur. Phys. J. B **52**, 345, (2006).

[40] A.C. Hewson, *The Kondo Problem to Heavy Fermions* (Cambridge University Press, Cambridge, 1993).

[41] N. E. Bickers, D. L. Cox, and J.W. Wilkins, Phys. Rev. B **36**, 2036 (1987); N. E. Bickers, Rev. Mod. Phys. **59**, 845 (1987).

[42] V. Zlatić, R. Monnier, and J. Freericks, Physica B: Physics of Condensed Matter **380-382**C, in press (2006)

[43] K. Hanzawa, K. Yamada, and K. Yosida, J. Magn. Magn. Mater. **47 & 48**, 357 (1985).

[44] In Kondo systems with small T_K the paramagnetic entropy is removed at $T_c > T_K$ by a magnetic phase transition. In such systems the low-temperature maximum of $\alpha(T)$ might be concealed and it will emerge only if the FL state is restored by pressure or magnetic field but these additional complications are neglected here.

[45] J. K. Freericks and V. Zlatić, Phys. Rev. B **58**, 322 (1998).

[46] J. K. Freericks, D. O. Demchenko, A. V. Joura, and V. Zlatić, Phys. Rev. B **68**, 195120 (2003).

[47] A. V. Joura, D. O. Demchenko, and J. K. Freericks, Phys. Rev. B **69**, 165105 (2004).

[48] M. J. Burns and P. M. Chaikin, Phys. Rev. B 27, 5924 (1983).

[49] I. Paul and G. Kotliar, Phys. Rev. B **64**, 184414 (2001).

[50] N. Kernavanois, S. Raymond, E. Ressouche, B. Grenier, and J. Flouquet, Phys. Rev. B **71**, 064404 (2005).

[51] Gignoux, D. and Gomez-Sal, J. C. Phys. Rev. B **30**, 3967–3973 (1984).

[52] See also discussion in Sec.IV.1, regarding the variation of $\alpha(T)$ induced by Ge-doping in $EuCu_2(Ge_{1-x}Si_x)_2$ for $x \simeq 1$.

[53] M. Kim, Y. Nakai, H. Tou, M. Sera, F. Iga, T. Takabatake and S. Kunii, J. Phys. Soc. Japan, **75**, 064704, 2006.

[54] S. Kobayashi, Y. Yoshino, S. Tsuji, M. Sera and F. Iga, J. Phys. Soc. Japan, **72**, 25, 2003.

[55] M. Očko, C. Geibel and F. Steglich Phys. Rev. B**64**, 195107 (2001)

[56] M. Očko, D. Drobac, B. Buschinger, C. Geibel and F. Steglich Phys. Rev. B**64**, 195106 (2001)

[57] M. Očko, J. L. Sarrao, I. Aviani, Dj. Drobac, .I. Ž ivković, and M. Prester. Phys. Rev. B**68**, 975102 (2003)

[58] V. Zlatić and J. Freericks, Acta Phys. Pol. B **34** (2003) 931.

[59] C. Dallera, M. Grioni, A. Shukla, G. Vank, J. L. Sarrao, J. P. Rueff, and D. L. Cox, Phys. Rev. Lett. **88**, 196403 (2002).

[60] D. Withoff, and E. Fradkin, Phys. Rev. Lett. **64**, 1835 (1990).

[61] S. Burdin and V. Zlatic, arXiv:cond-mat/0212222 (2002).

[62] J. N. Hancock, T. McKnew, Z. Schlesinger J. L. Sarrao, and Z. Fisk, Phys. Rev. Lett. **92**, 186405 (2004).

[63] J.L. Sarrao, Physica B, **259 - 261**, 129 (1999).